Ion Crystals and Liquids in Penning Traps

John Bollinger
NIST-Boulder
Ion storage group

Wayne Itano, David Wineland, Jospeh Tan, Pei Huang, Brana Jelenkovic, Travis Mitchell, Brad King, Jason Kriesel, Marie Jensen, Taro Hasegawa, Nobuysau Shiga, Michael Biercuk, Hermann Uys, Joseph Britton, Dan Dubin – UCSD(theory)

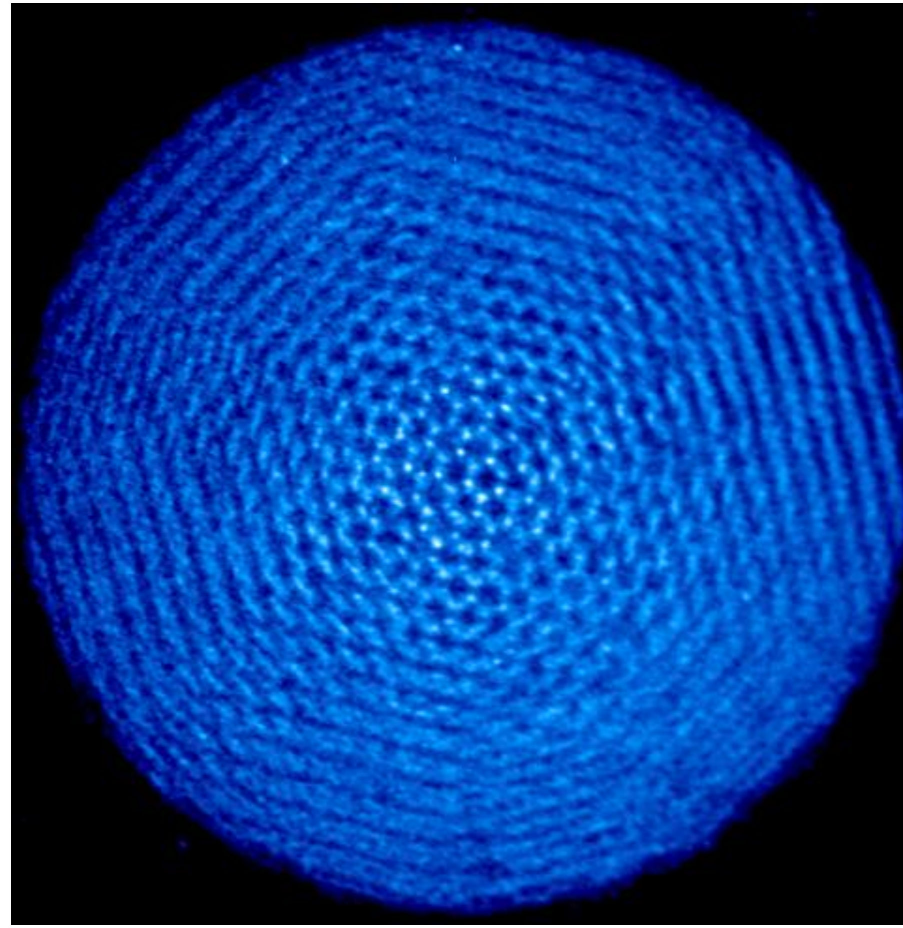

Outline:

Introduction:

Penning traps – how do they work, thermal equilibrium, one-component plasmas, strong correlation

- Observation of crystalline structure:

  Bragg scattering, real imaging, structural phase transitions

- Modes

→ No quantum mechanics; everything in this talk uses classical physics

→ Please ask questions!!

→ Ref: Dubin and O'Neil, Rev. Mod. Physics **71**, 87 (1999)

Types of traps in atomic physics

Rf or Paul Trap
RF & DC
Voltages

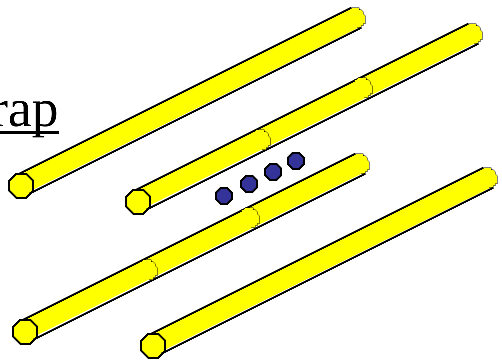

Penning Trap
(or Penning-
Malmberg trap)
DC Voltages &
Static B-Field

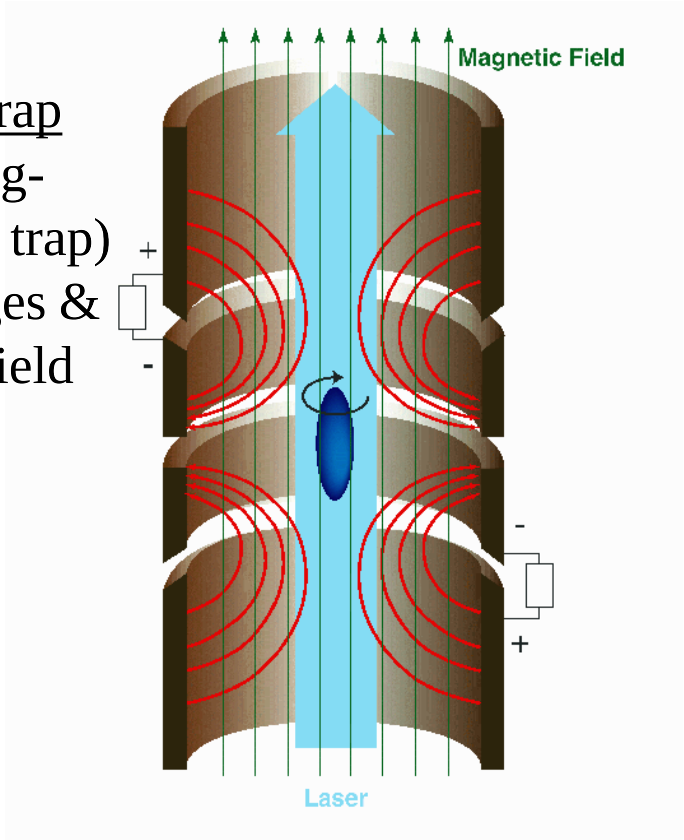

(see Monroe lectures)

good for tight confinement and laser cooling smaller numbers of particles

good for laser cooling larger numbers of particles

Penning –Malmberg traps

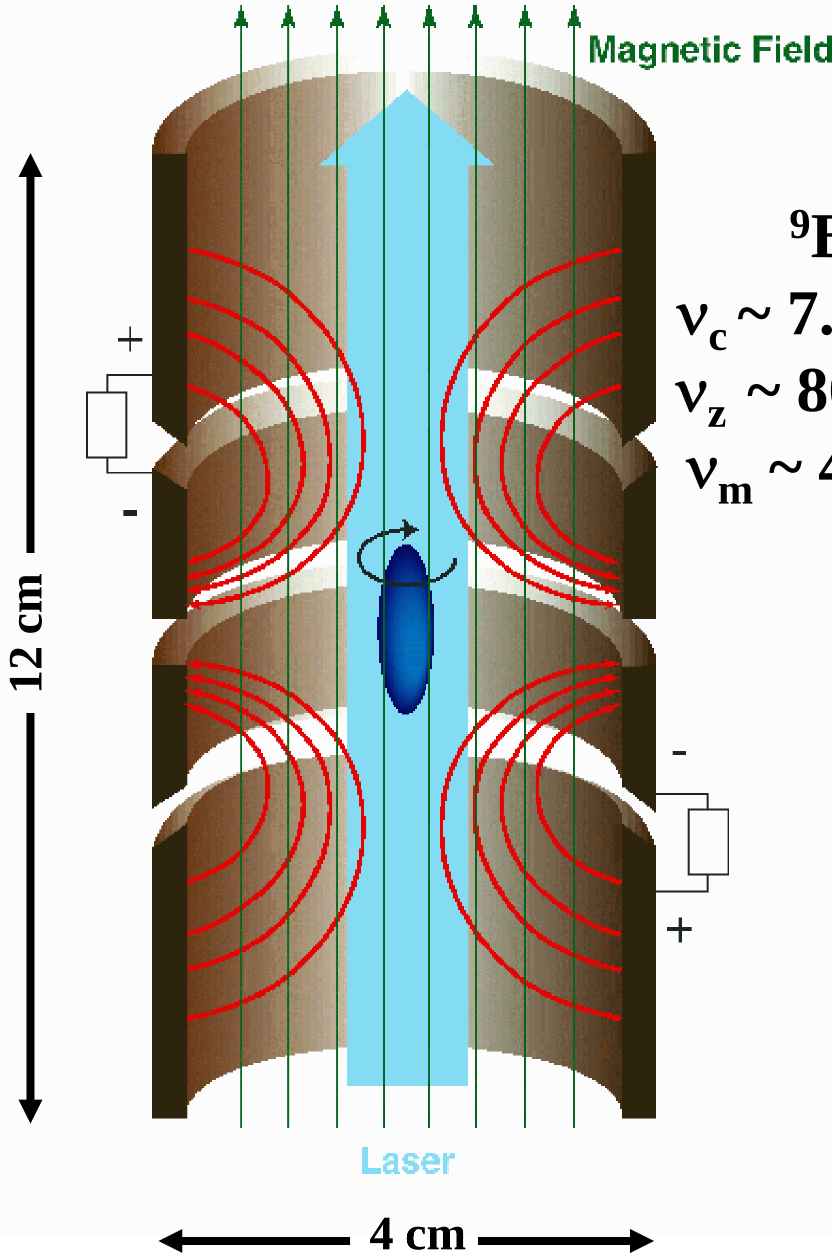

$^9Be^+$

$\nu_c \sim 7.6$ MHz

$\nu_z \sim 800$ kHz

$\nu_m \sim 40$ kHz

- g-factors, atomic phys. – U of Wash., Mainz, Imperial College, NIST, ..
- mass spectroscopy – U of Wash., Harvard, ISOLDE/CERN, …
- cluster studies – Mainz/Griefswald
- non-neutral plasmas – UCSD, Berkeley, Princeton, NIST, …
- anti-matter – UCSD, Harvard, CERN, Swansea, …
- quantum information/simulation – NIST, Imperial College, Harvard, Mainz/Ulm, ….

Single particle motion in a Penning trap

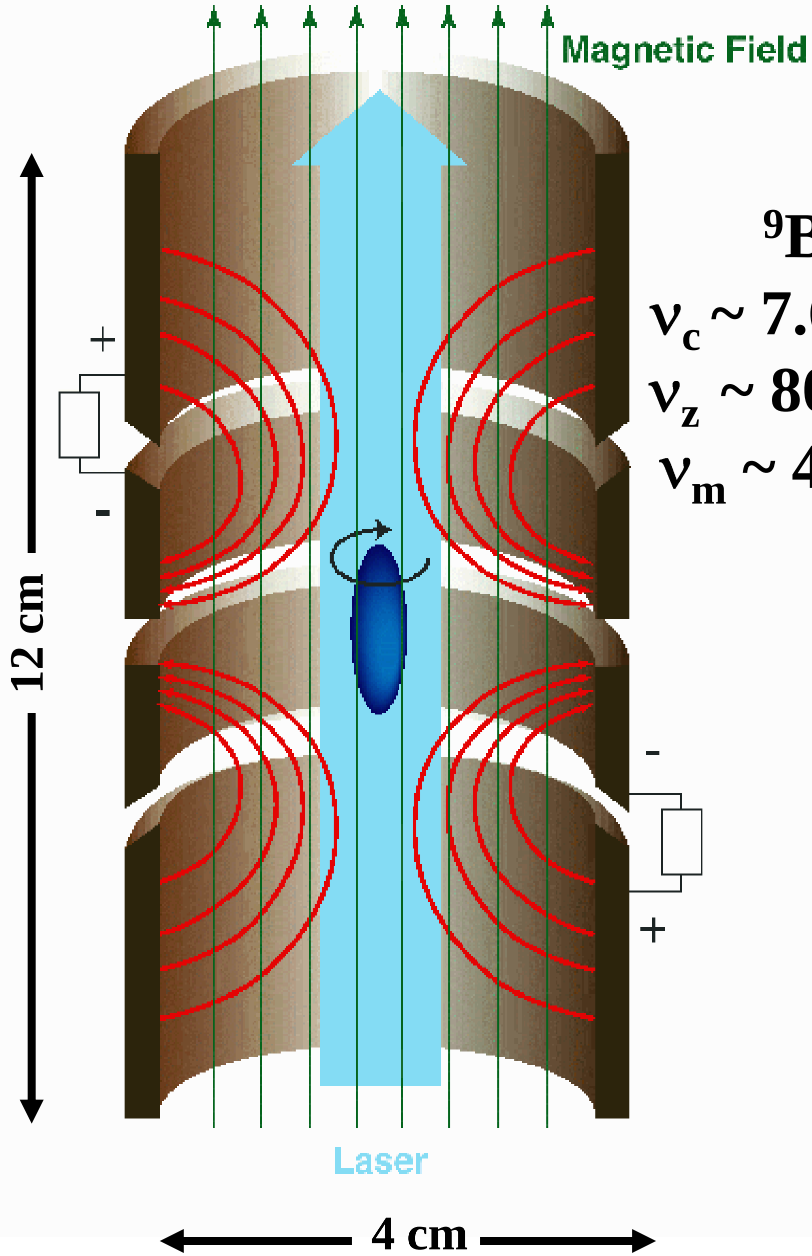

$^9Be^+$

$\nu_c \sim 7.6$ MHz

$\nu_z \sim 800$ kHz

$\nu_m \sim 40$ kHz

For $r, z <<$ trap dimensions,

$$\varphi_{trap}(r,z) \approx \frac{1}{2} m\omega_z^{\;2}\left(z^2 - \frac{r^2}{2}\right)$$

$$z(t) = z_o \sin(2\pi\nu_z t + \varphi_z)$$

$$r(t) = r_c \sin\left(2\pi(\nu_c - \nu_m)t + \phi_c\right) + r_m \sin(2\pi\nu_m t + \phi_m)$$

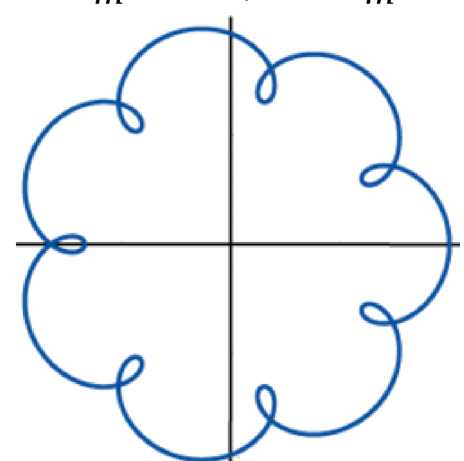

Confinement in a Penning trap

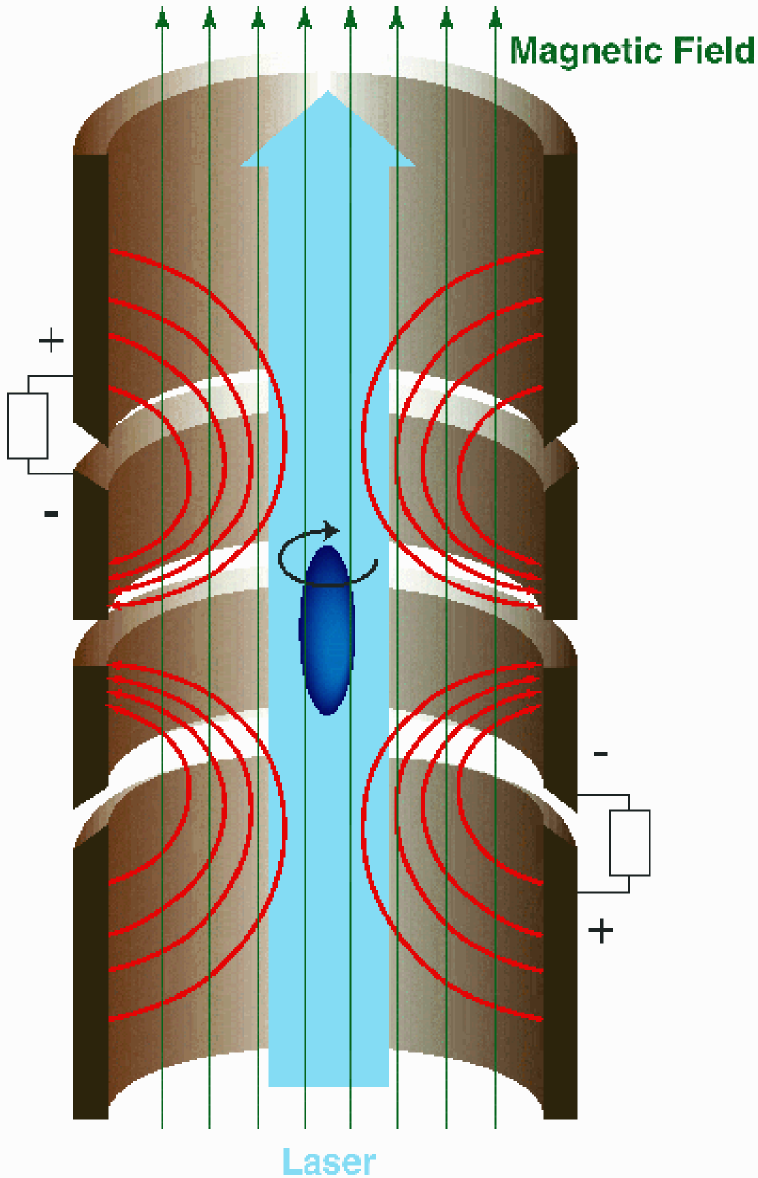

axial confinement $\leftrightarrow$
conservation of energy

radial confinement $\leftrightarrow$
conservation of angular momentum

$$P_\theta = \sum_j \left(m v_{\vartheta_j} + \frac{q}{c} A_\theta(r_j) \right) r_j$$

$$\approx \frac{qB}{2c} \sum_j r_j^{\,2} \text{ for } A_\theta(r) = \frac{Br}{2} \text{ and } B \text{ large}$$

$\Rightarrow$ axial asymmetries important -
magnetic field tilt

radial confinement due to rotation –
ion plasma rotates $v_\theta = \omega_r r$ due to ***ExB*** fields

in rotating frame, $v_\theta \hat{\theta} \times B\hat{z}$ Lorentz force is
directed radially inward

NIST Penning trap

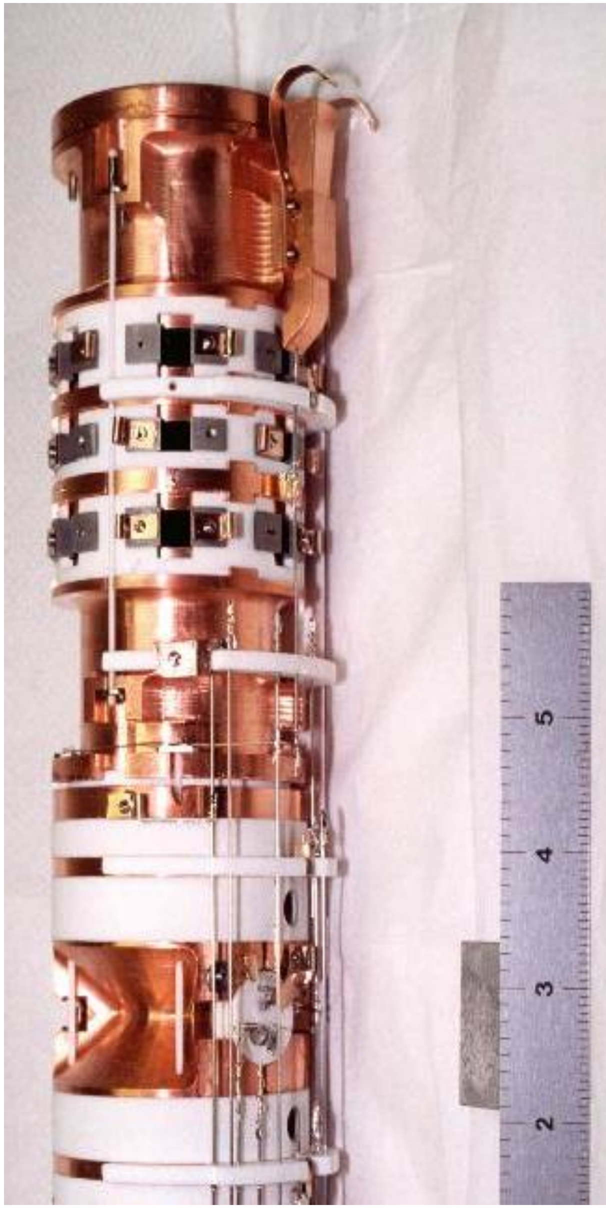

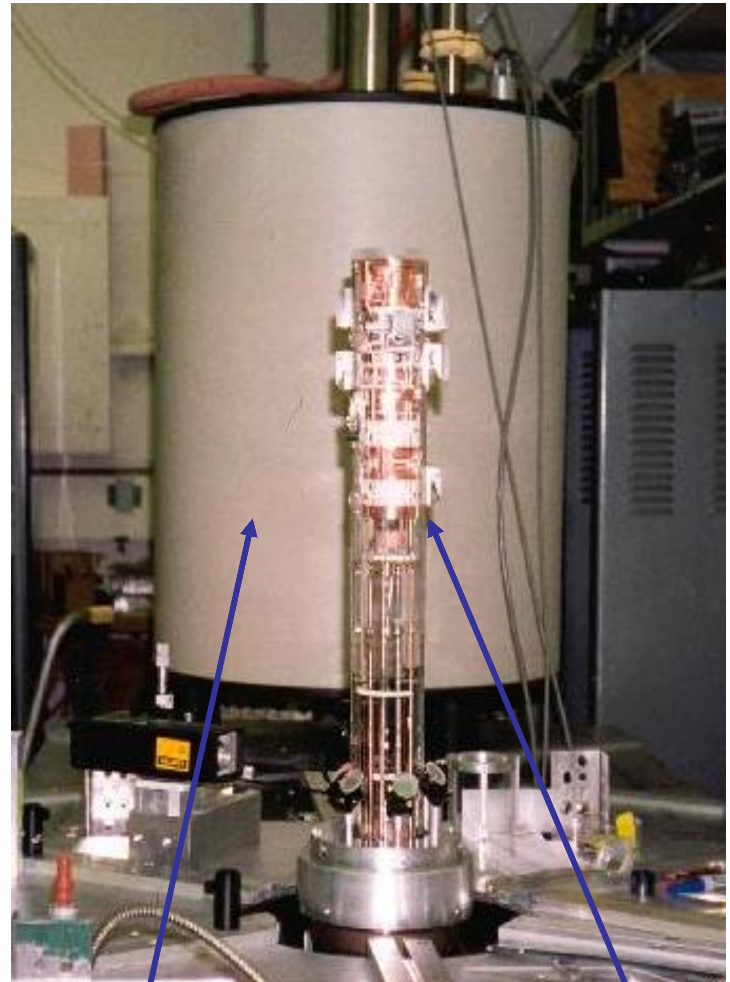

4.5 Tesla
Super Conducting
Solenoid

Quartz
Vacuum envelope
$P < 10^{-10}$ Torr

Non-neutral plasmas in traps evolve into **bounded thermal equilibrium states**

thermal equilibrium, Hamiltonian and total canonical angular momentum conserved $\Rightarrow$

$$f(\mathbf{r},\mathbf{v}) \propto \exp[-(h+\omega_r p_\theta)/k_B T]$$

where $h = \frac{m\mathbf{v}^2}{2} + e\phi(\mathbf{r})$ and $p_\theta = m\mathrm{v}_\theta \mathrm{r} + \frac{eB}{2c}\mathrm{r}^2$

$$f(\mathbf{r},\mathbf{v}) \propto n(\mathrm{r},\mathrm{z}) \exp[-\frac{m}{2k_B T}(\underbrace{\mathbf{v}+\omega_r \mathrm{r}\hat{\theta}}_{\text{plasma rotates rigidly at frequency } \omega_r})^2]$$

density distribution

plasma rotates rigidly at frequency ω_r

$$n(\mathrm{r},\mathrm{z}) \propto \exp\{-\frac{1}{k_B T}[e\phi_p(\mathrm{r},\mathrm{z}) + e\phi_T(\mathrm{r},\mathrm{z}) + m\omega_r(\Omega_c - \omega_r)\frac{r^2}{2}]\}$$

Ω_c = eB/mc = cyclotron frequency

plasma potential

trap potential

Lorentz force potential

centrifugal potential

Lorentz-force potential gives radial confinement !!

Equilibrium plasma properties

thermal equilibrium $\Rightarrow$ rigid rotation ω_r

- **$T \sim 0$ $\Rightarrow$ constant plasma density,**
  $n_o = 2\varepsilon_o m\omega_r(\Omega_c-\omega_r)/e^2$,
  Ω_c = cyclotron frequency
  plasma density $\rightarrow$ 0 over a Debye length $\lambda_D = [k_BT/(4\pi n_o e^2)]^{1/2}$

- **quadratic trap potential, $e\phi_T \sim m\omega_z^2(z^2-r^2/2) \Rightarrow$ plasma shape is a spheroid**

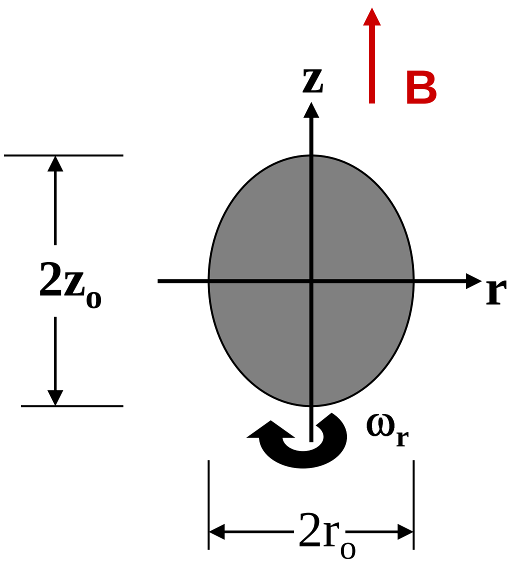

aspect ratio $\alpha \equiv z_o/r_o$
determined by ω_r

$$\frac{\omega_z^2}{2\omega_r(\Omega_c-\omega_r)} = Q_1{}^0\left[\frac{\alpha}{(\alpha^2-1)^{1/2}}\right]/(\alpha^2-1)^{1/2}$$

associated Legendre function

Plasma aspect ratio determined by ω_r

$$\frac{\omega_z^2}{2\omega_r(\Omega_c-\omega_r)} = \frac{Q_1{}^0\left[\frac{\alpha}{(\alpha^2-1)^{1/2}}\right]}{(\alpha^2-1)^{1/2}}$$

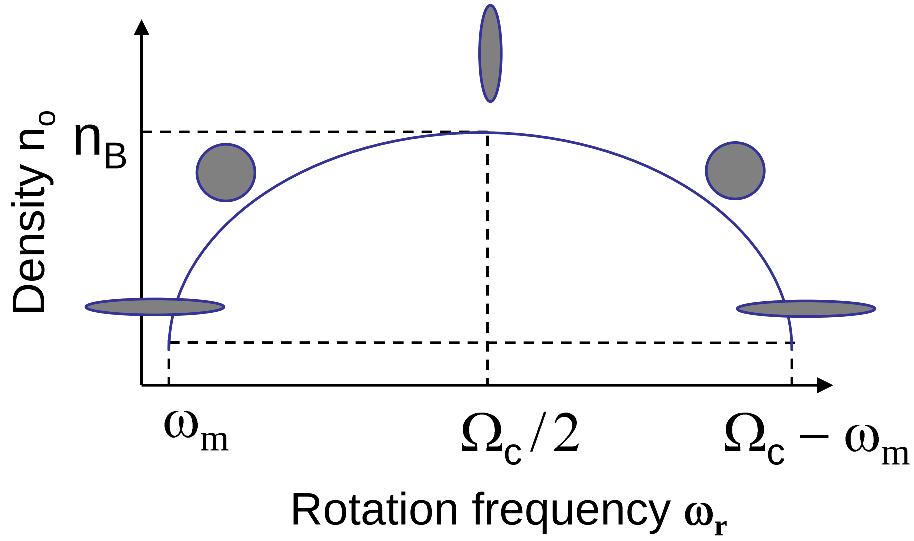

experimental measurements of plasma shape vs ω_r

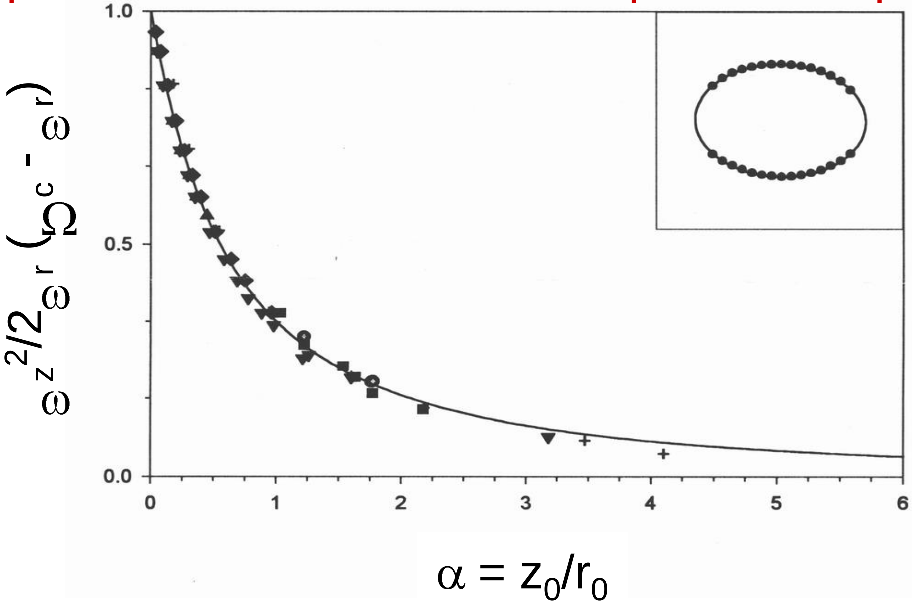

Simple equilibrium theory describes the plasma shapes

Ions in a trap are an example of a one component plasma

one component plasma (OCP) – consists of a single species of charged particles immersed in a neutralizing background charge

ions in a trap are an example of an OCP (Malmberg and O'Neil PRL 39, (77))

$$n(\mathsf{r},\mathsf{z}) \propto \exp\{-\tfrac{1}{k_B T}[e\phi_p(\mathsf{r},\mathsf{z}) + e\phi_T(\mathsf{r},\mathsf{z}) + m\omega_r(\Omega_c - \omega_r)\tfrac{r^2}{2}]\}$$

looks like neutralizing background

$$\nabla^2\{\phi_T(\mathsf{r},\mathsf{z}) + \tfrac{1}{e}m\omega_r(\Omega_c - \omega_r)\tfrac{r^2}{2}\} = -4\pi e n_{bkgnd}$$

$$n_{bkgnd} = -\frac{m\omega_r(\Omega_c - \omega_r)}{2\pi e^2}$$

thermodynamic state of an OCP determined by:

$$\Gamma \equiv \frac{q^2}{a_{WS} k_B T}, \quad \frac{4}{3}\pi a_{WS}{}^3 n \equiv 1 \qquad \Gamma \approx \frac{\text{potential energy between neighboring ions}}{\text{ion thermal energy}}$$

$\Gamma > 1 \Rightarrow$ strongly coupled OCP

Why are strongly coupled OCP's interesting?

Strongly coupled OCP's are models of dense astrophysical matter – example: outer crust of a neutron star

For an infinite OCP, $\Gamma > 2 \Rightarrow$ **liquid behavior**
$\Gamma \sim 173 \Rightarrow$ **liquid-solid phase transition to bcc lattice**

Brush, Salin, Teller (1966) $\Gamma \sim 125$
Hansen (1973) $\Gamma \sim 155$
Slatterly, Doolen, DeWitt(1980) $\Gamma \sim 168$
Ichimaru; DeWitt; Dubin (87-93) $\Gamma \sim 172\text{-}174$

Coulomb energies/ion of bulk bcc, fcc, and hcp lattices differ by $< 10^{-4}$

body centered cubic

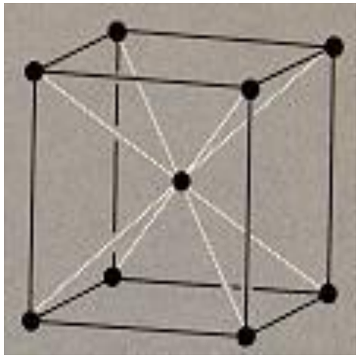

face centered cubic

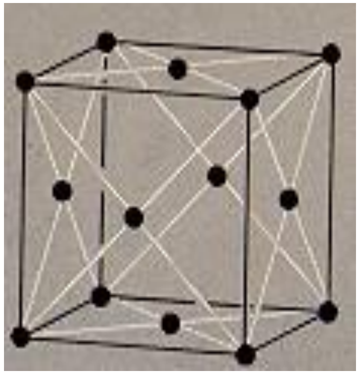

hexagonal close packed

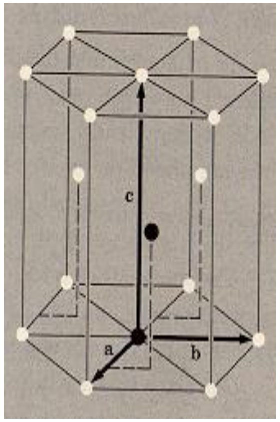

with trapped ions, $n_o \sim 10^9\ \mathrm{cm}^{-3}$ $\Rightarrow$ $\Gamma > 500$
$T < 5\ \mathrm{mK}$

Plasmas vs strongly coupled plasmas

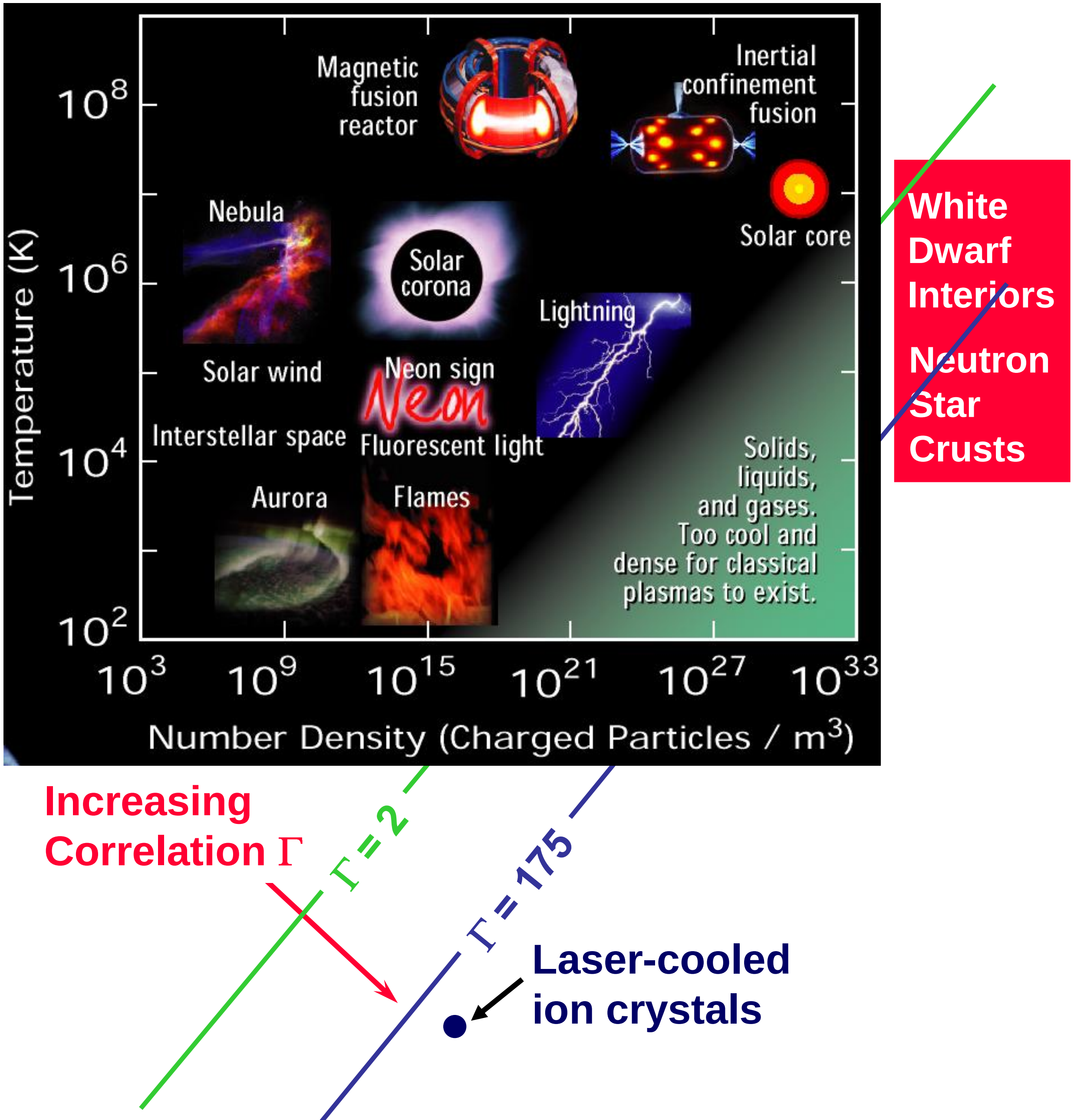

How large must a plasma be to exhibit a bcc lattice?

1989 - Dubin, planar model PRA 40, 1140 (89)

result: plasma dimensions ≥ 60 interparticle spacings required for bulk behavior

$N > 10^5$ in a spherical plasma ⇒ bcc lattice

2001 – Totsji, simulations, spherical plasmas, N≤120 k

PRL 88, 125002 (2002)

result: N>15 k in a spherical plasma ⇒ bcc lattice

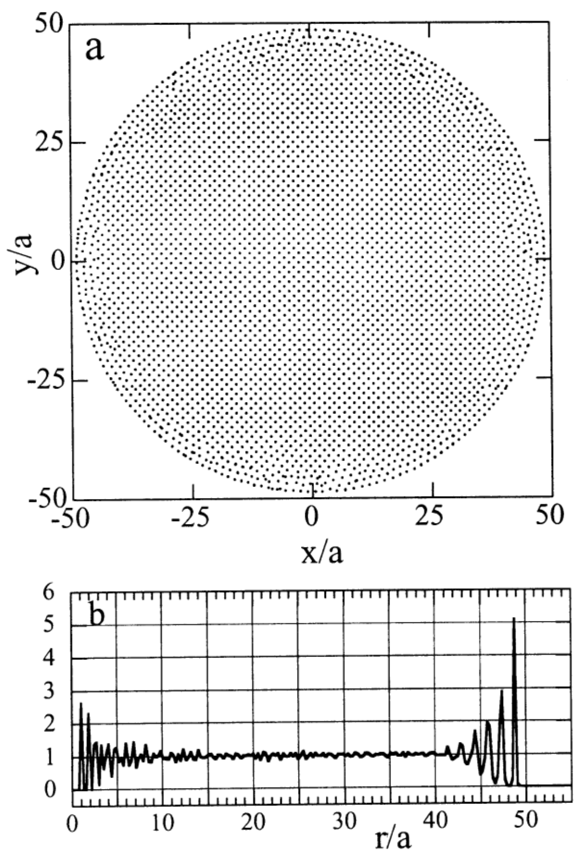

Experimental techniques:

Doppler laser cooling and resonance fluorescence detection

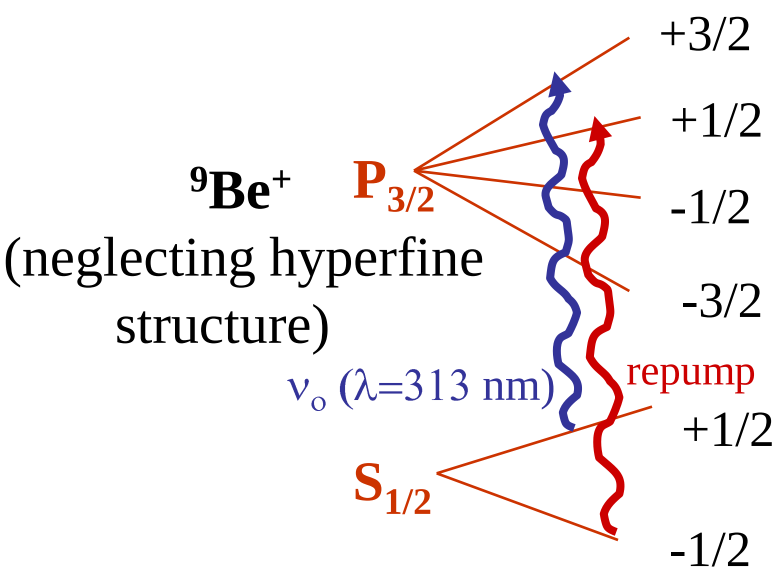

$T_{min}(^9Be^+) \sim 0.5$ mK

$T_{measured} < 1$ mK

Laser torque

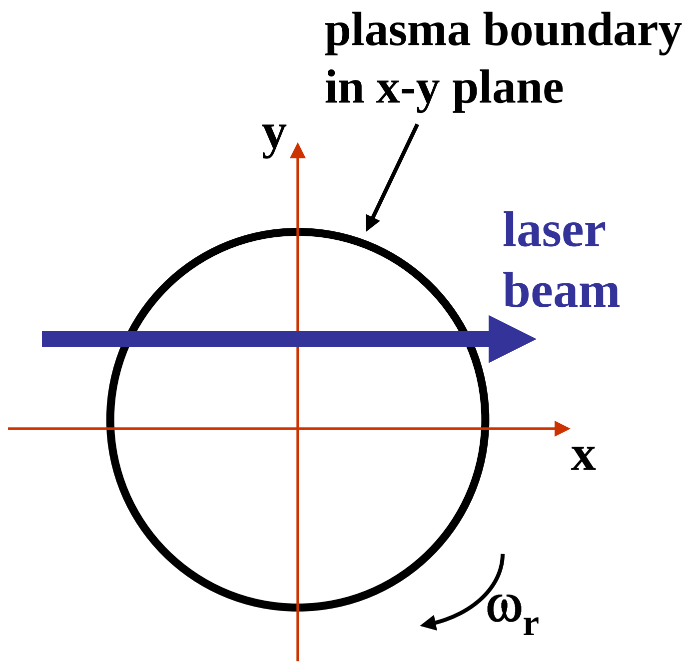

The laser beam position and frequency control the torque and ω_r

With the laser beam directed as shown, increasing torque $\Rightarrow$ increasing ω_r $\Rightarrow$ decreasing radius

Evidence for bcc crystals: Bragg scattering

$f_{rotation}$ = 240 kHz
n = 7.2 x 10^8 /cm^3

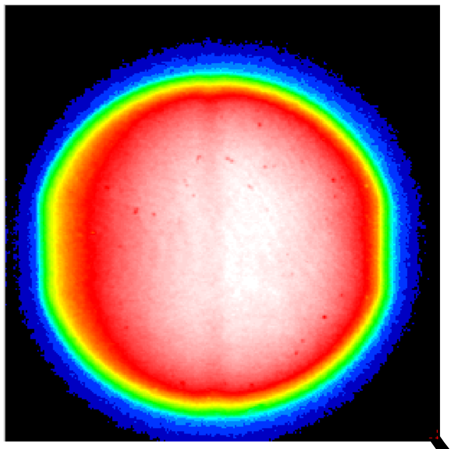

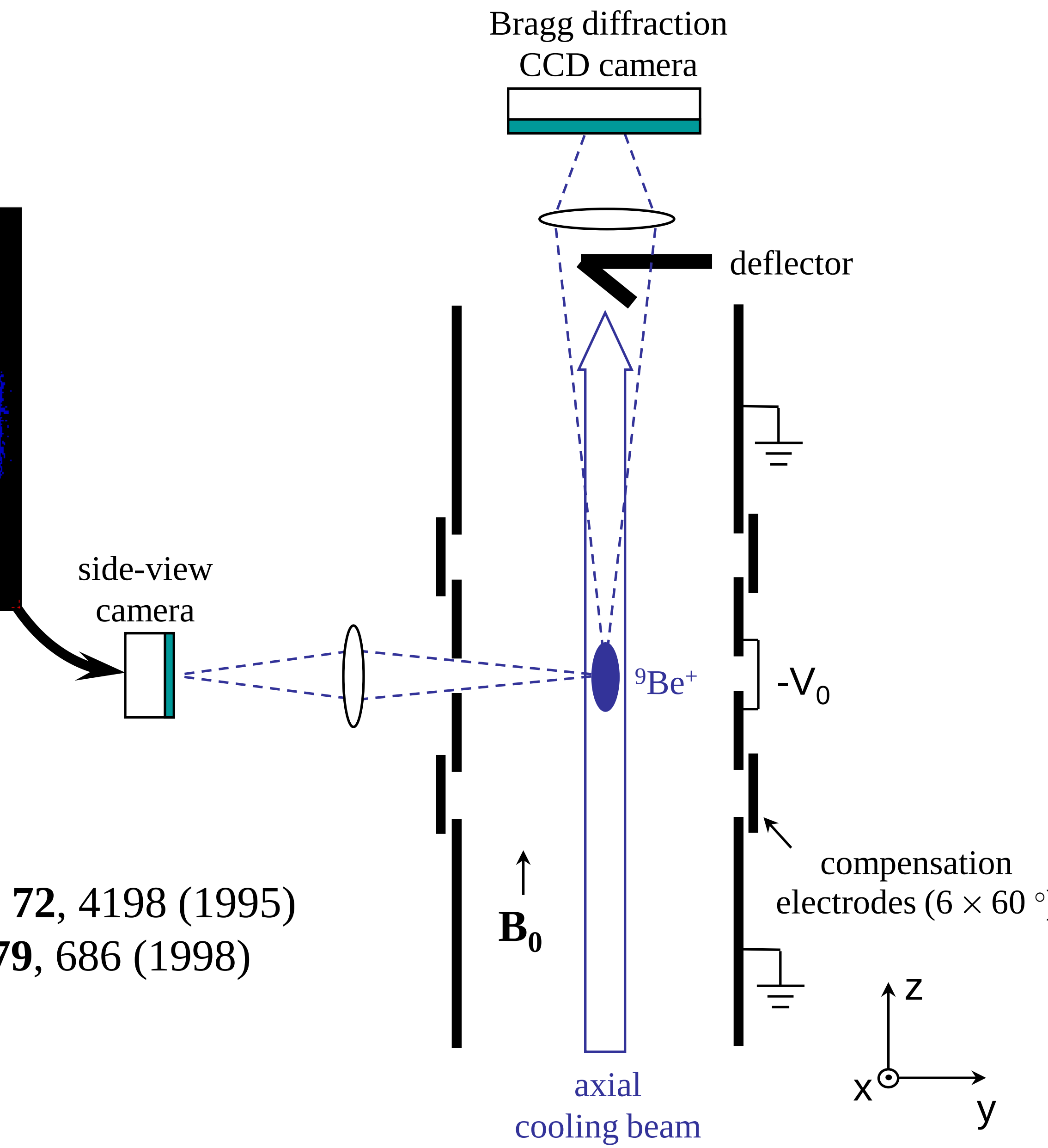

J.N. Tan, *et al.*, Phys. Rev. Lett. **72**, 4198 (1995)
W.M. Itano, *et al.*, Science **279**, 686 (1998)

Bragg scattering from spherical plasmas with N~ 270 k ions

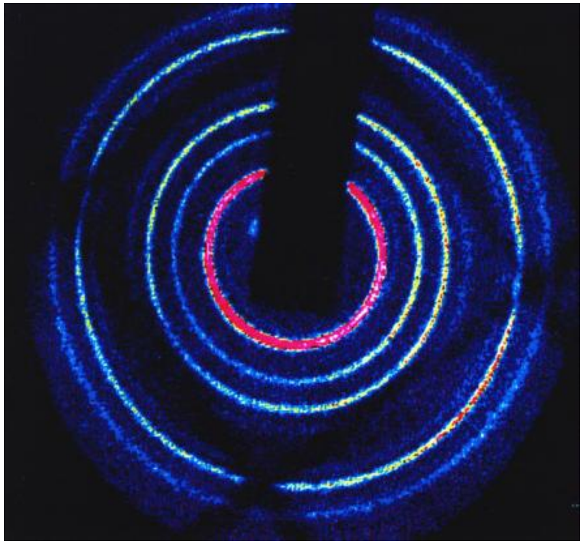

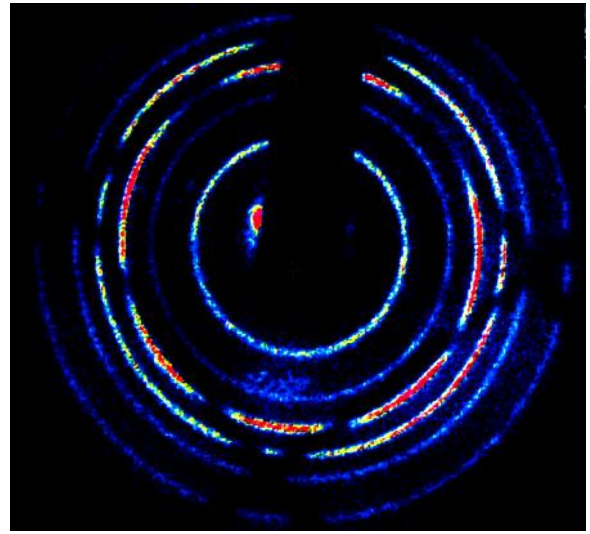

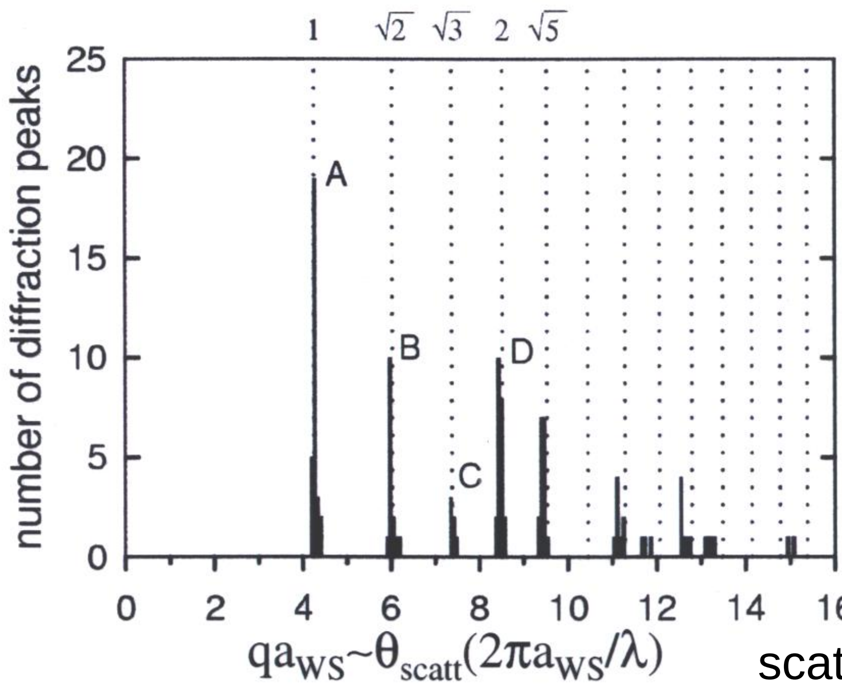

scattering angle →

Evidence for
bcc crystals

Rotating wall control of the plasma rotation frequency

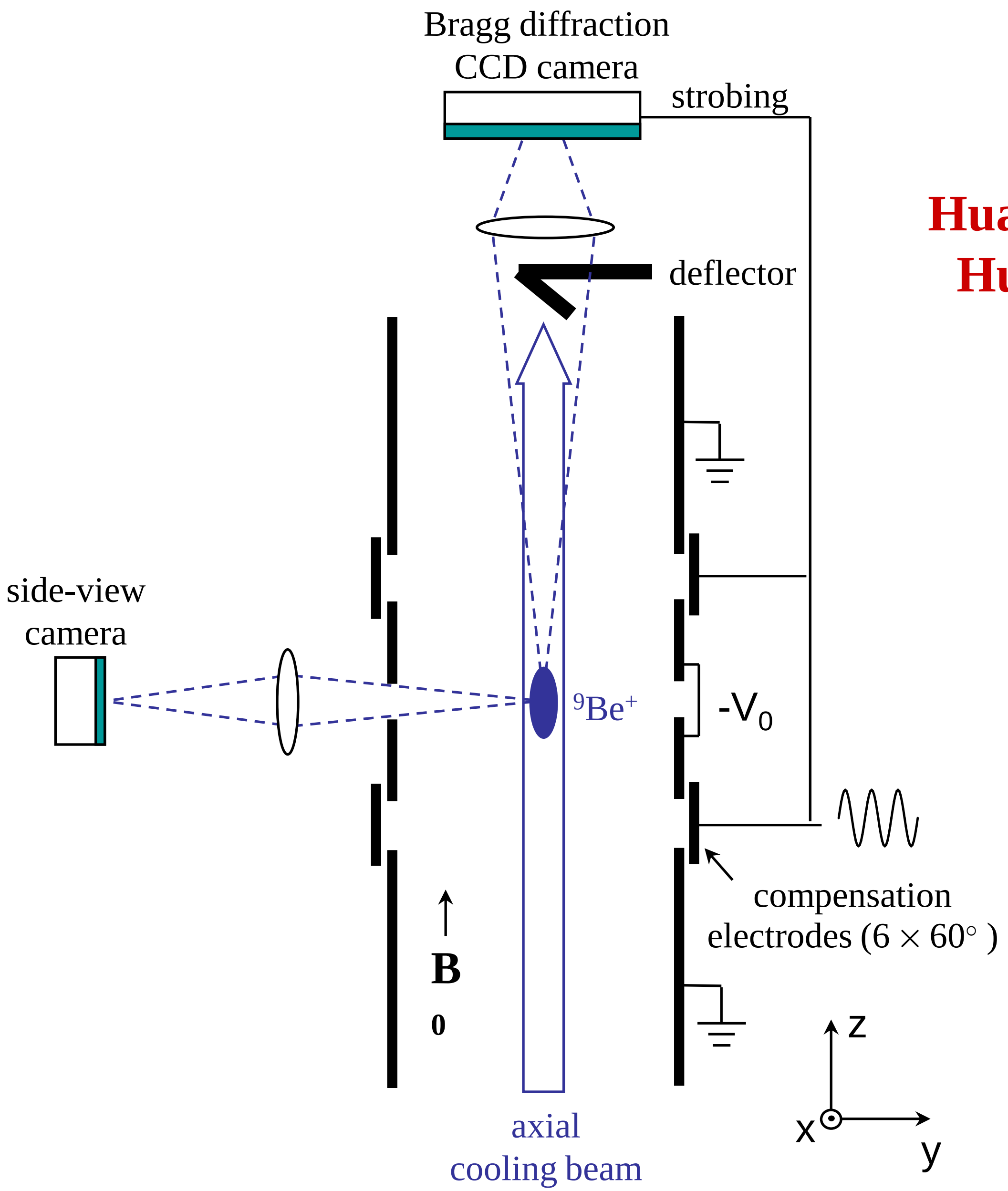

Huang, *et al.* (UCSD), PRL 78, 875 (97)
Huang, *et al.* (NIST), PRL 80, 73 (98)

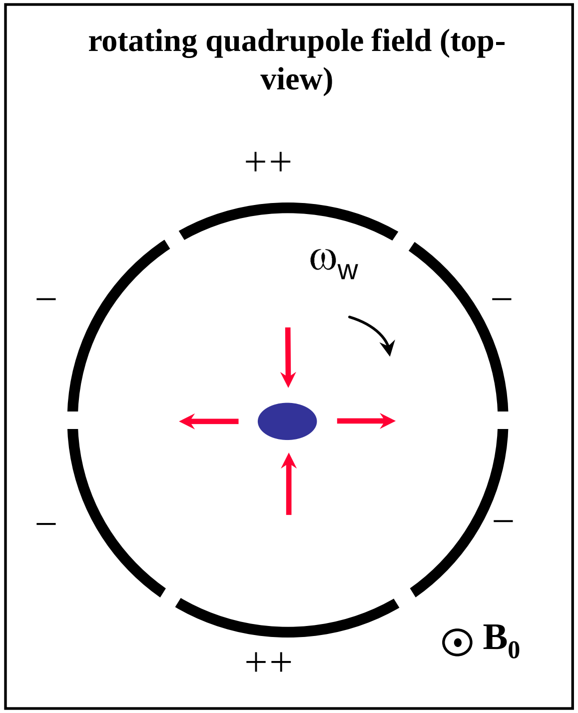

Phase-locked control of the plasma rotation frequency

Huang, *et al.*, Phys. Rev. Lett. 80, 73 (98)

time averaged Bragg scattering

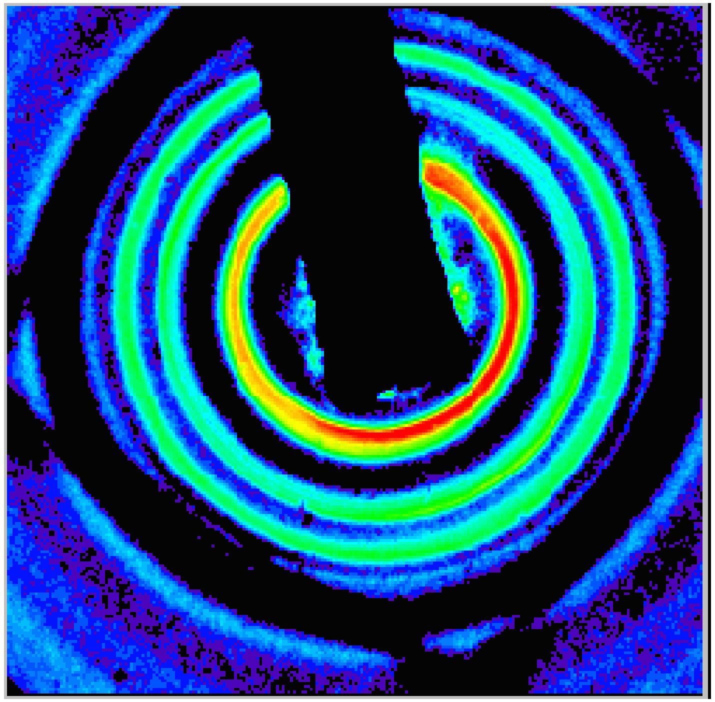

camera strobed by the rotating wall

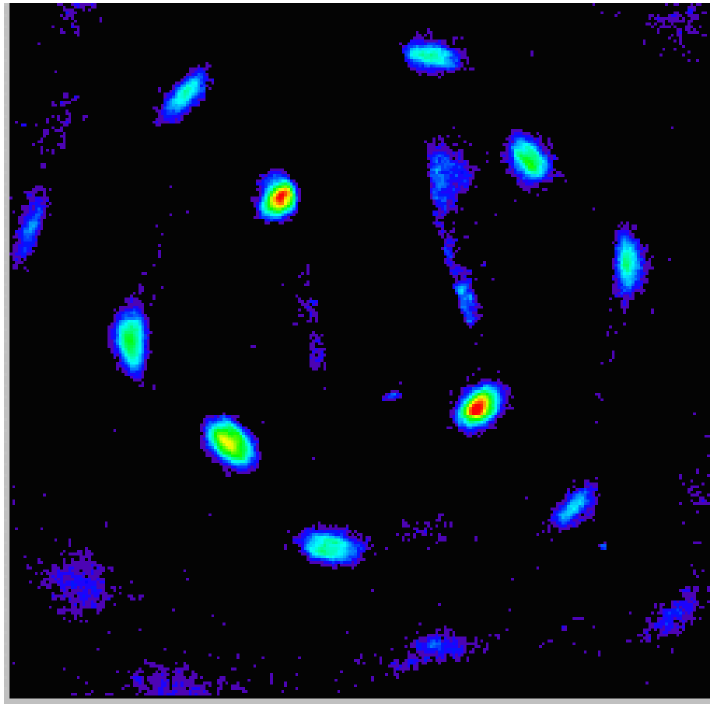

N > 200,000 ions ⇒ always observe bcc crystalline patterns

- 100,000> N > 20,000 ⇒ observe fcc, hcp?, in addition to bcc

Real space imaging

Mitchell. *et al.*, Science **282**, 1290 (98)

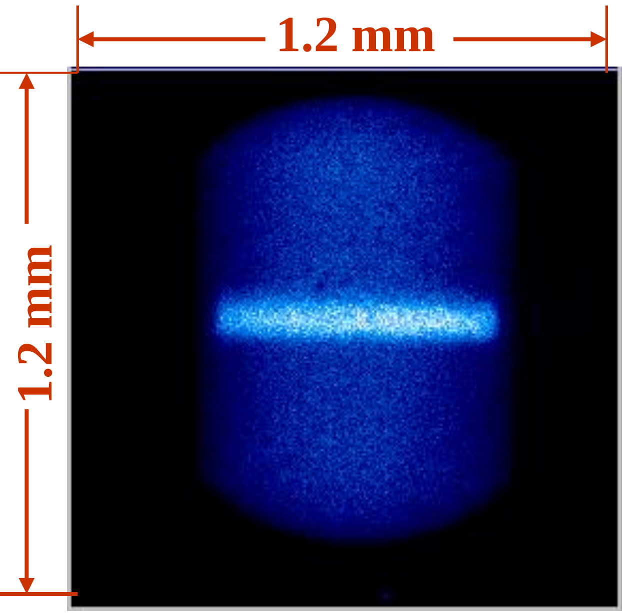

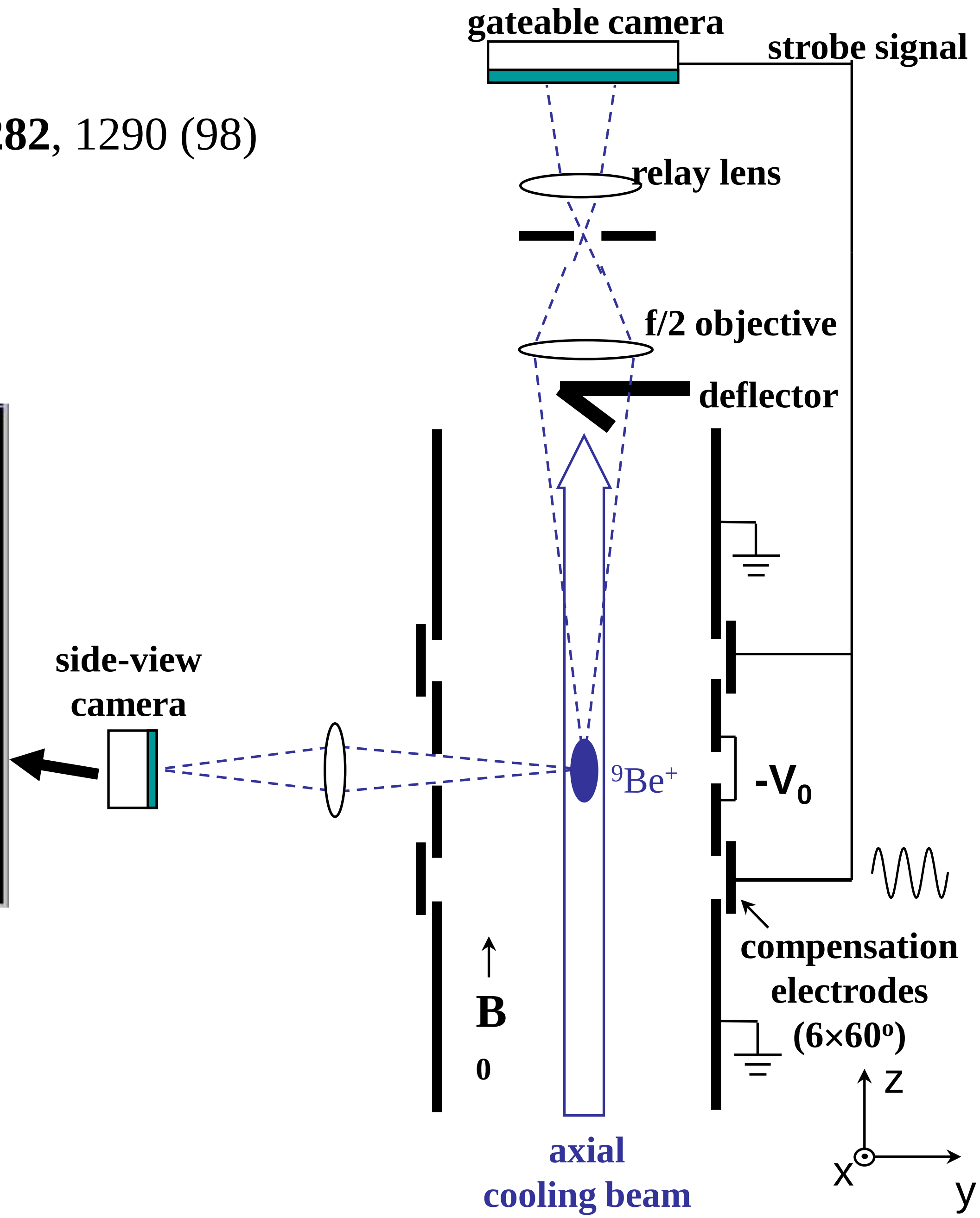

Top-view images in a spherical plasma of ~180,000 ions

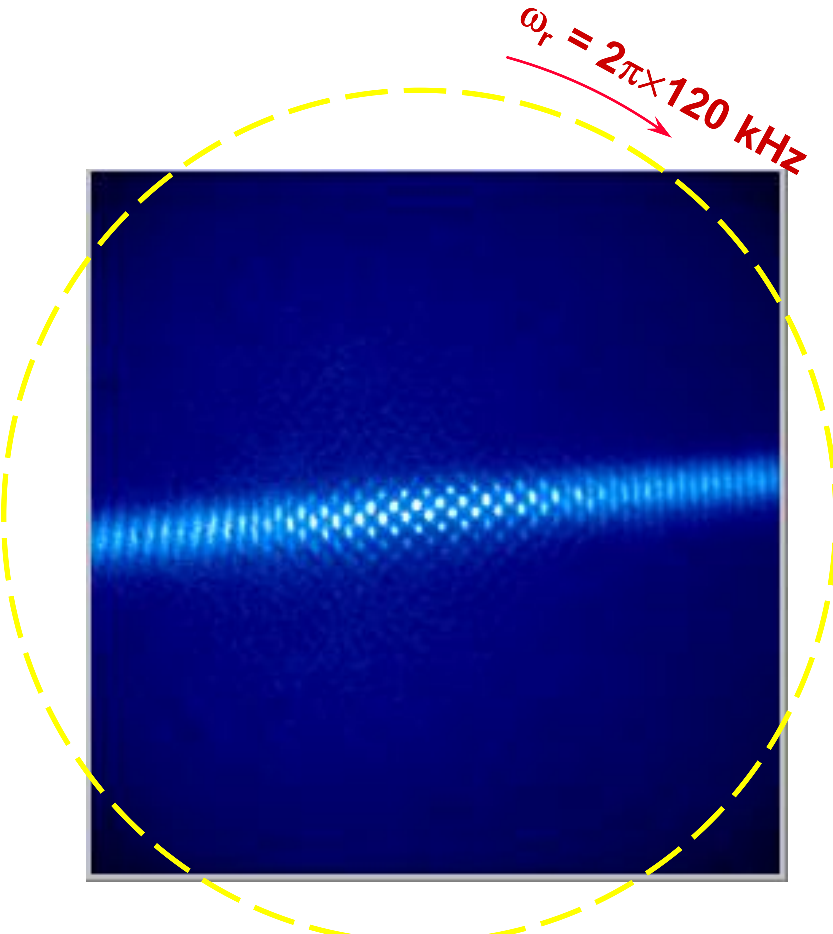

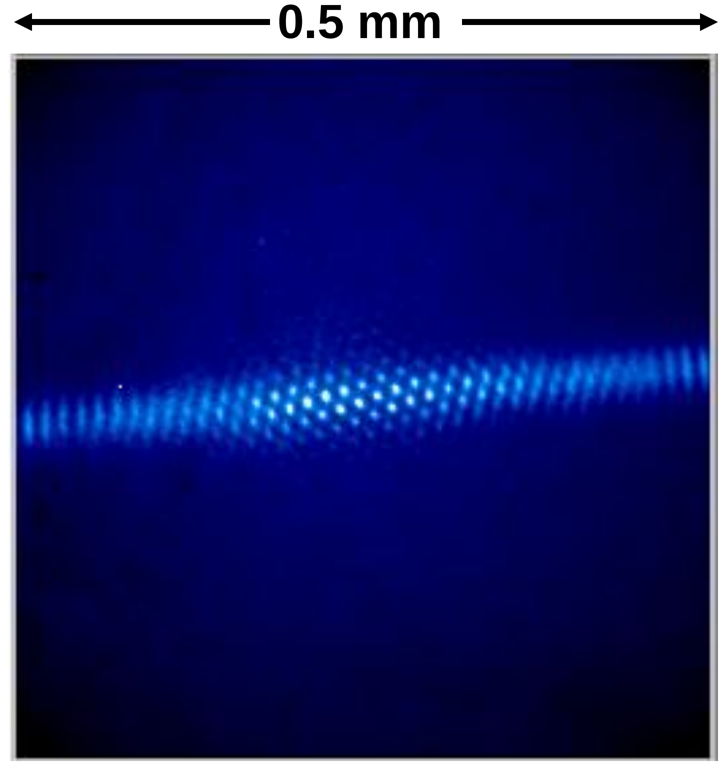

bcc (100) plane
predicted spacing: 12.5 μm
measured: 12.8 ± 0.3 μm

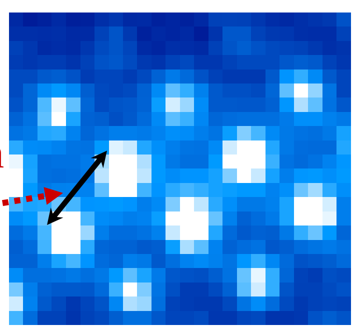

bcc (111) plane
predicted spacing: 14.4 μm
measured: 14.6 ± 0.3 μm

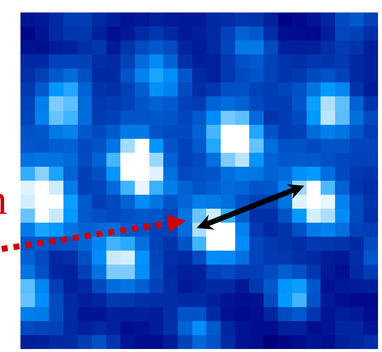

Real-space images with planar plasmas

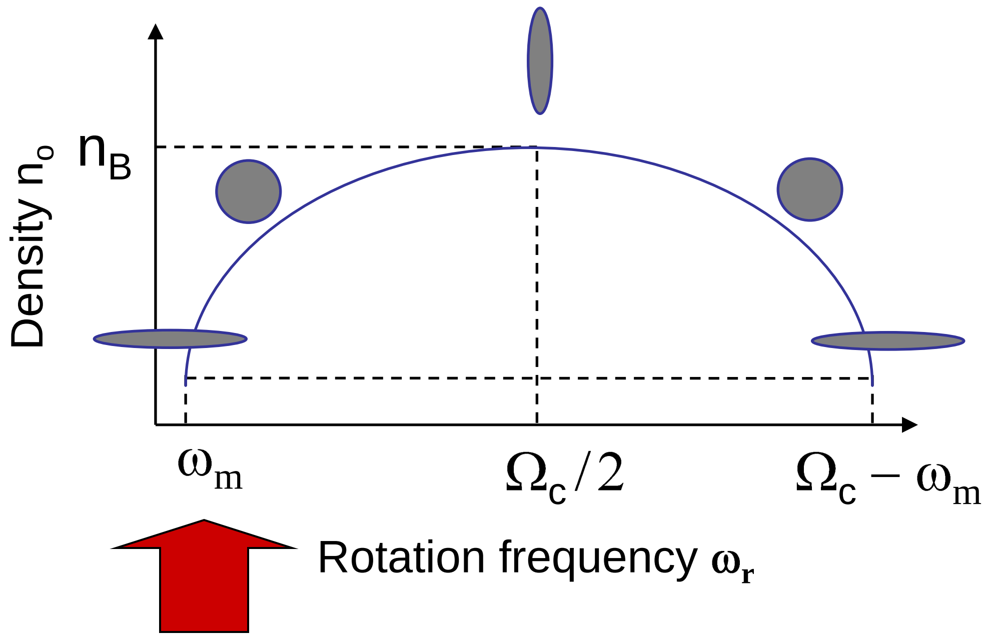

with planar plasmas all the ions can reside within the depth of focus

Planar plasmas: observation of structural phase transitions

top-views

65.70 kHz

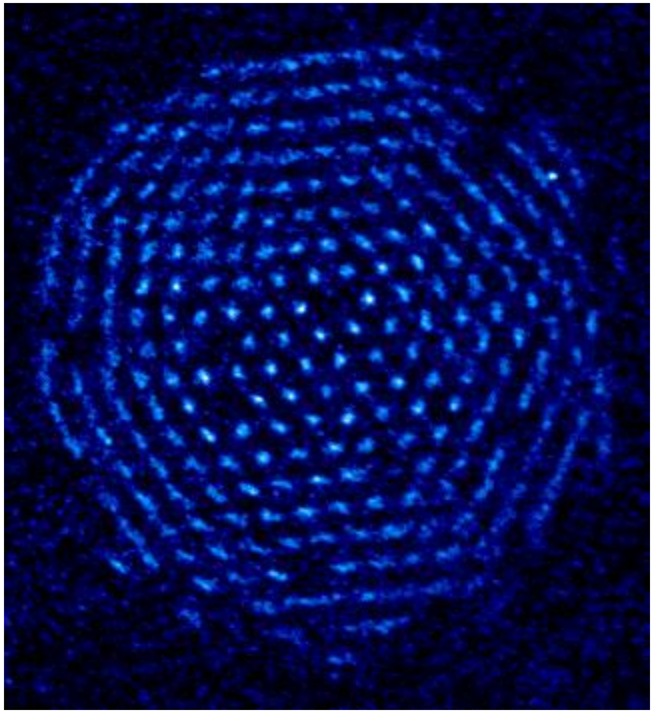

66.50 kHz

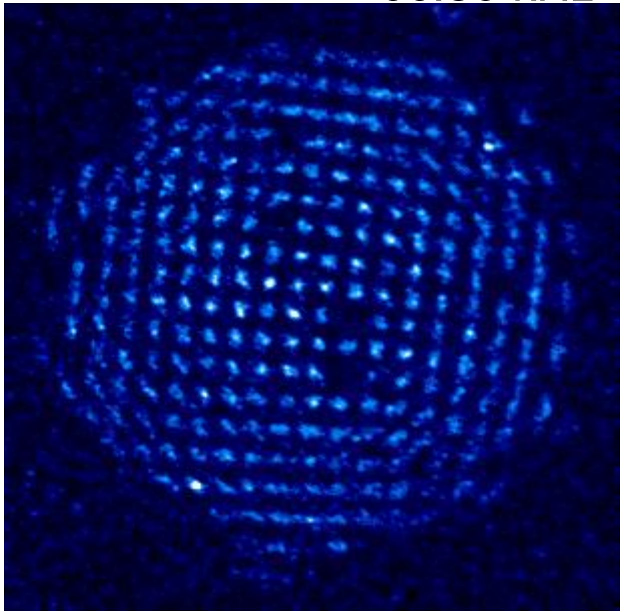

side-views

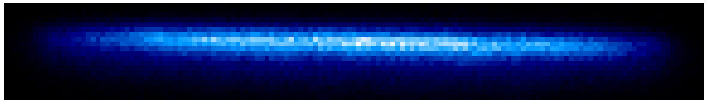

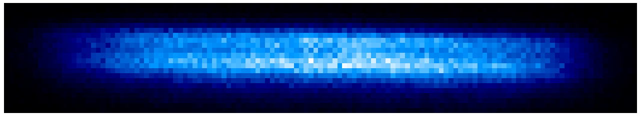

1 lattice plane, hexagonal order

used in current quantum information experiments

2 planes, cubic order

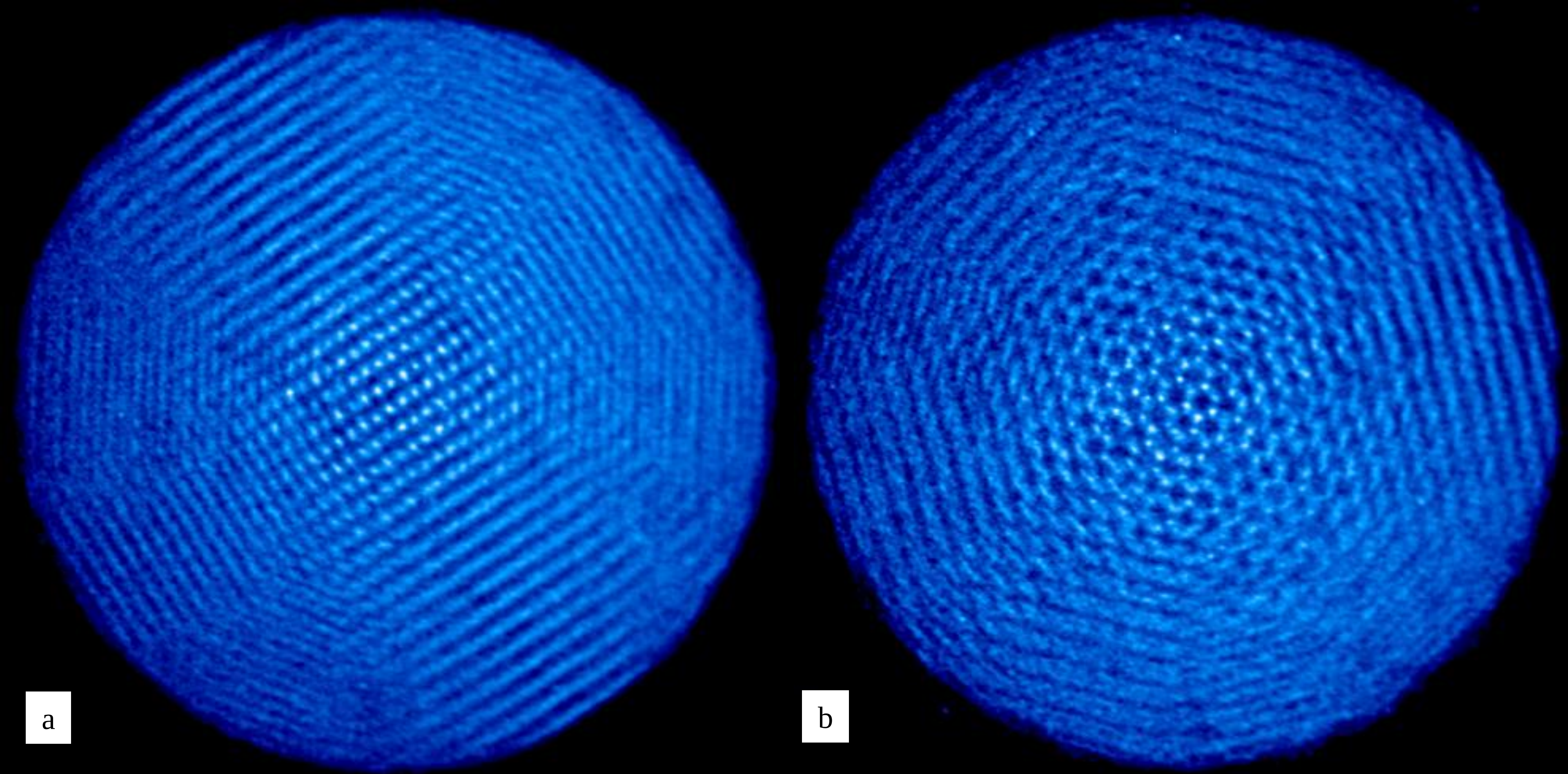

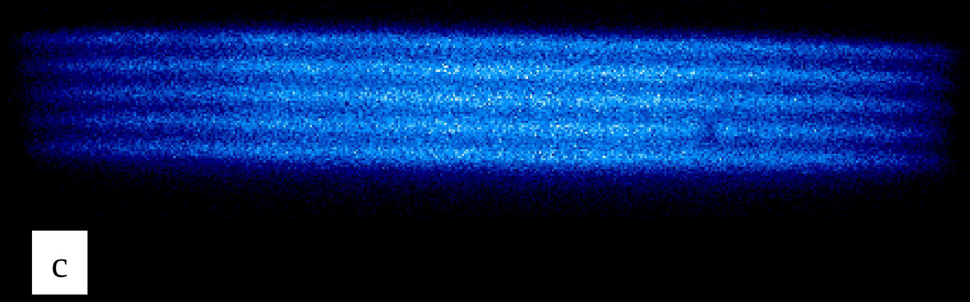

Top- (a,b) and side-view (c) images of crystallized $^{9}Be^{+}$ ions contained in a Penning trap. The energetically favored phase structure can be selected by changing the density or shape of the ion plasma. Examples of the (a) staggered rhombic and (b) hexagonal close packed phases are shown.

Mitchell, *et al.*, Science **282**, 1290 (98)

Theoretical curve from Dan Dubin, UCSD

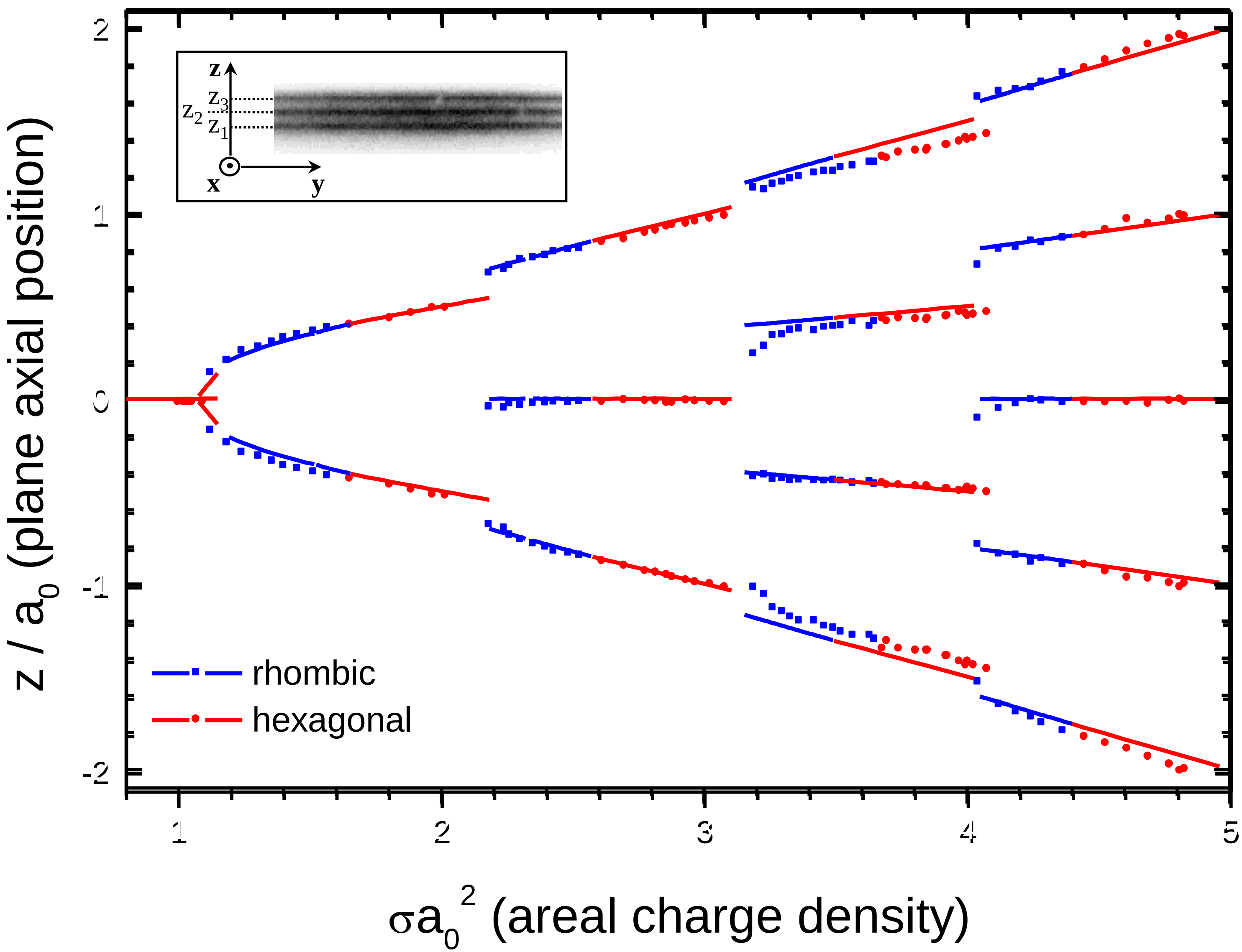

increasing rotation frequency →

Stick-slip motion of the crystal rotation

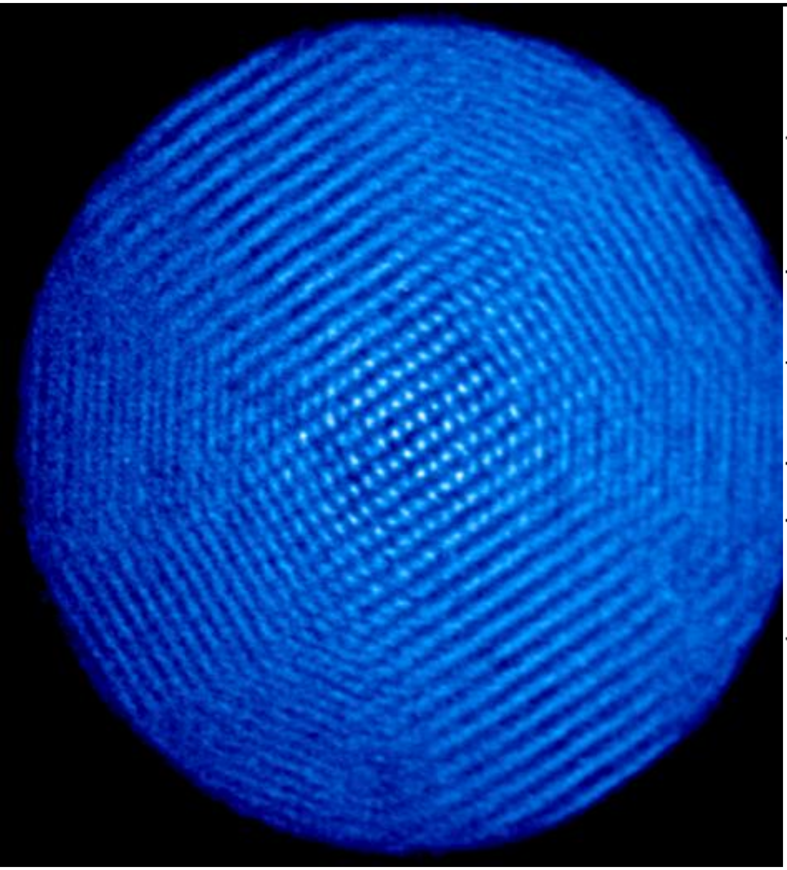

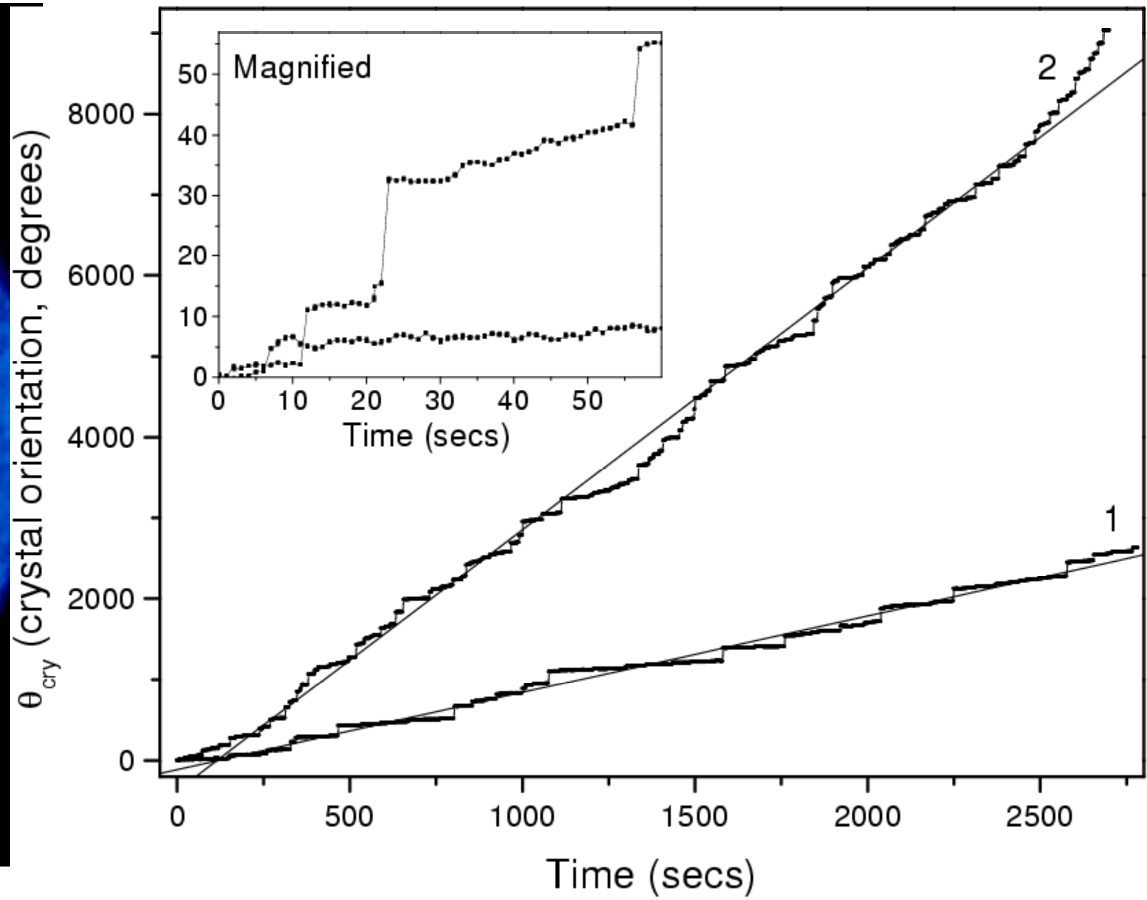

not a true phase lock!

- **frequency offset (ω_r-ω_{wall}) due to creep of 2 -18 mHz**
- **regions of phase-locked separated by sudden slips in the crystal orientation**
- **stick-slip motion due to competition between ⊥ laser and rotating wall torques**
- **mean time between slips ~10 s; what triggers the slips?**

Summary of crystal observations

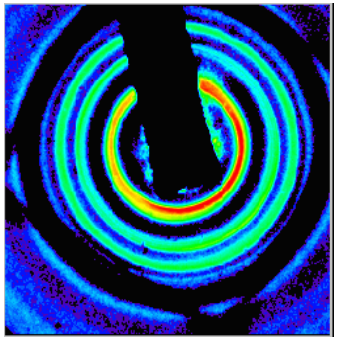

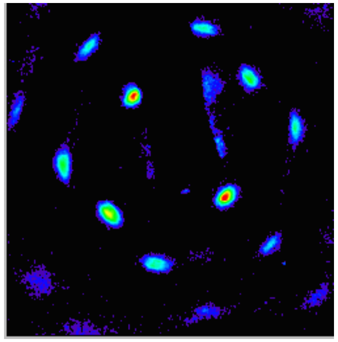

spherical plasmas

bcc crystals observed with N > 200 k ions

other crystal types (fcc, hcp) observed for 20 k < N <200 k

shell structure observed for N < 20 k ions

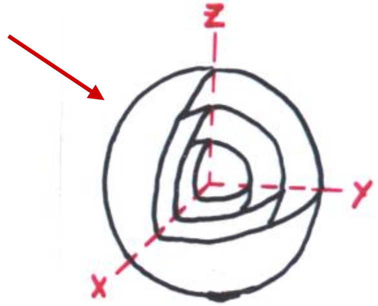

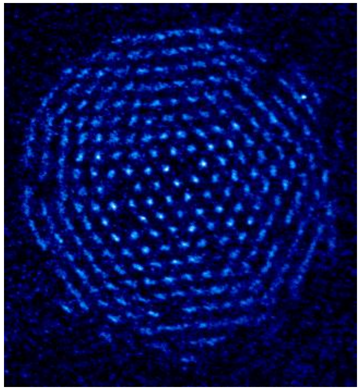

planar plasmas

structural phase transitions between rhombic planes (bcc-like)
and hexagonal planes (fcc-like or bcc-like)

good agreement with the predicted T=0 minimum energy lattice
for plasmas < 10 lattice planes thick

Modes of magnetized spheroidal plasmas

Detailed understanding of the plasma modes necessary for quantum information exps

Analytical cold fluid mode theory by Dan Dubin, PRL **66**, 2076 (1991);
accurate for mode wavelength >> interparticle spacing

Mode geometry characterized by l and m (indices of associated Legendre functions)

m is azimuthal mode number, (l-m) gives number of zeros along boundary

For given (l,m), many different modes exist: [2(l-m) + 2] l-m even
[2(l-m) + 1] l-m odd

l=1 modes are the COM excitations

(l=1, m=0)↔ axial COM mode ω_z

(1,1)↔ cyclotron COM mode $\Omega_c - \omega_m$
magnetron COM mode ω_m

l=2 modes are quadrupole deformations

(2,0) ↔
axial stretch mode

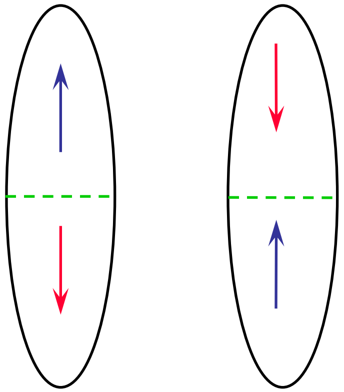

Doppler imaging of plasma mode velocities

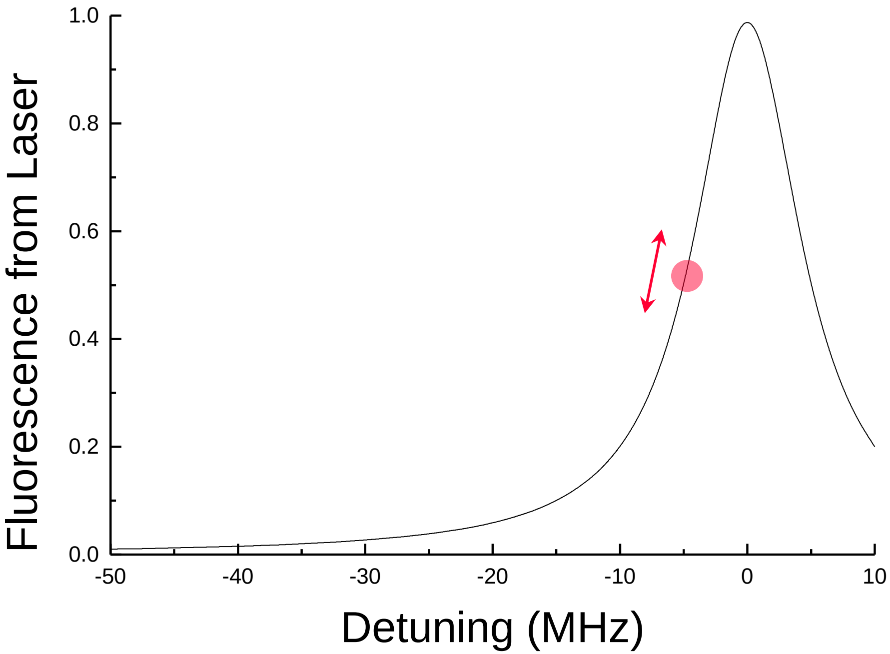

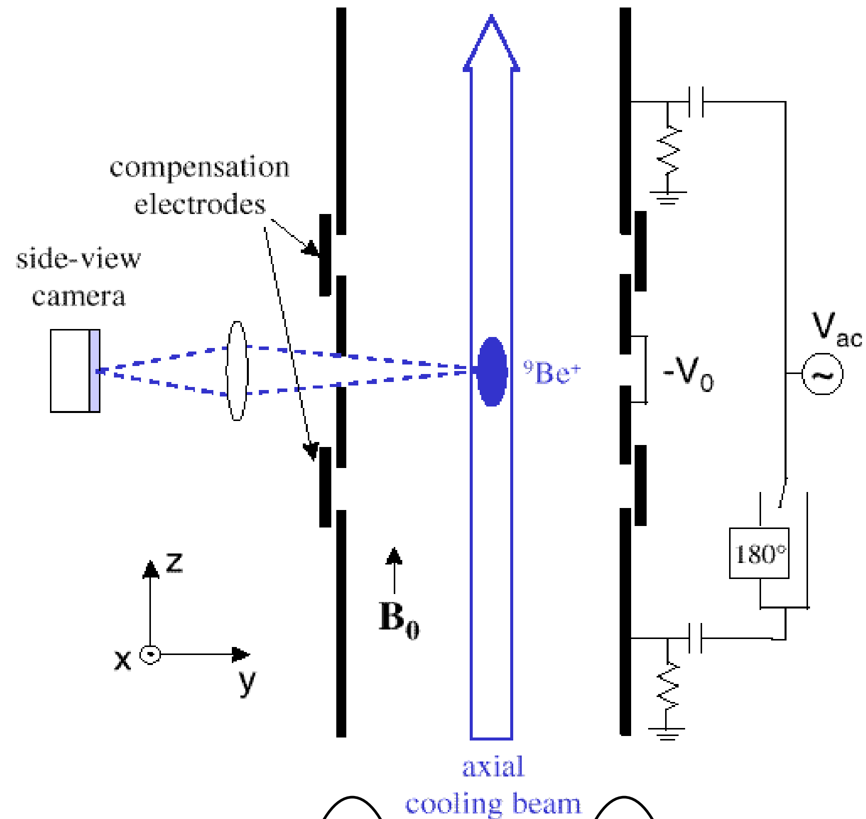

Modes can be detected and easily identified at low (linear) amplitudes

Detectable velocities < 0.5 m/sec corresponding to < 100 nm displacements (Biercuk et al., arXiv:1004.0780, 18 nm axial COM excitation excited with ~170 yN oscillating force.)

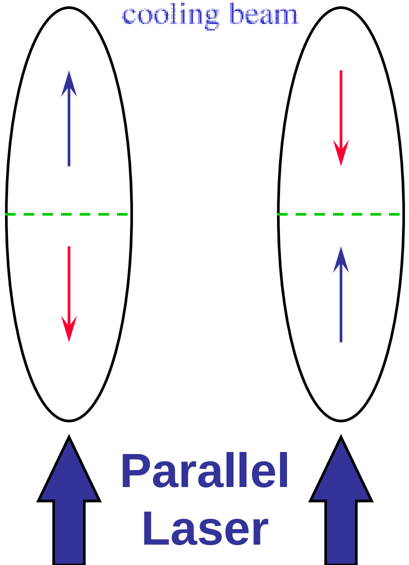

(2,0) mode excitation

$\omega_{2,0} = 2\pi \cdot 1.656$ MHz

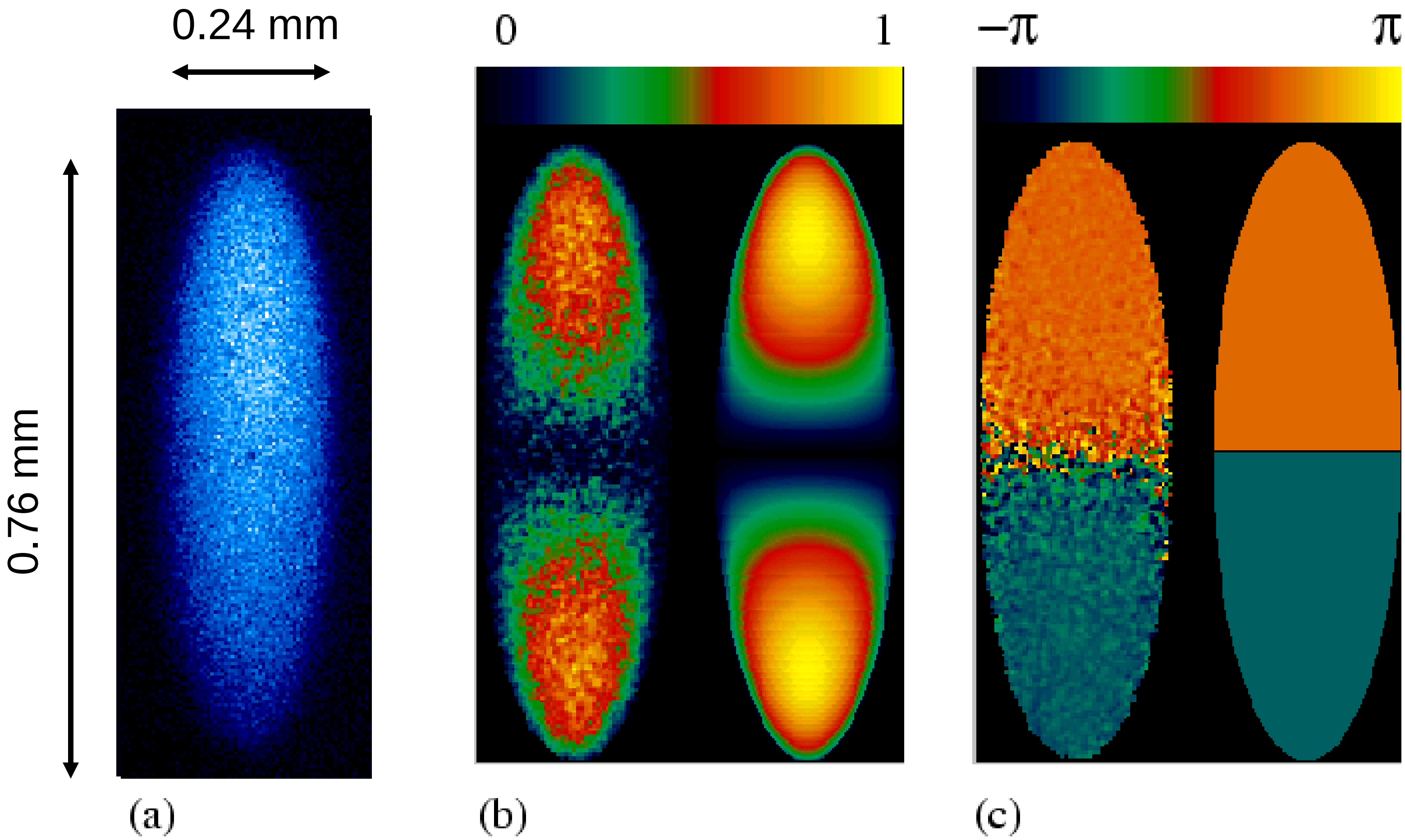

side-view image　　mode amplitude　　mode phase

Good agreement between theory and experiment !

(9,0) mode excitation

$\omega_{9,0} = 2\pi \cdot 2.952$ MHz

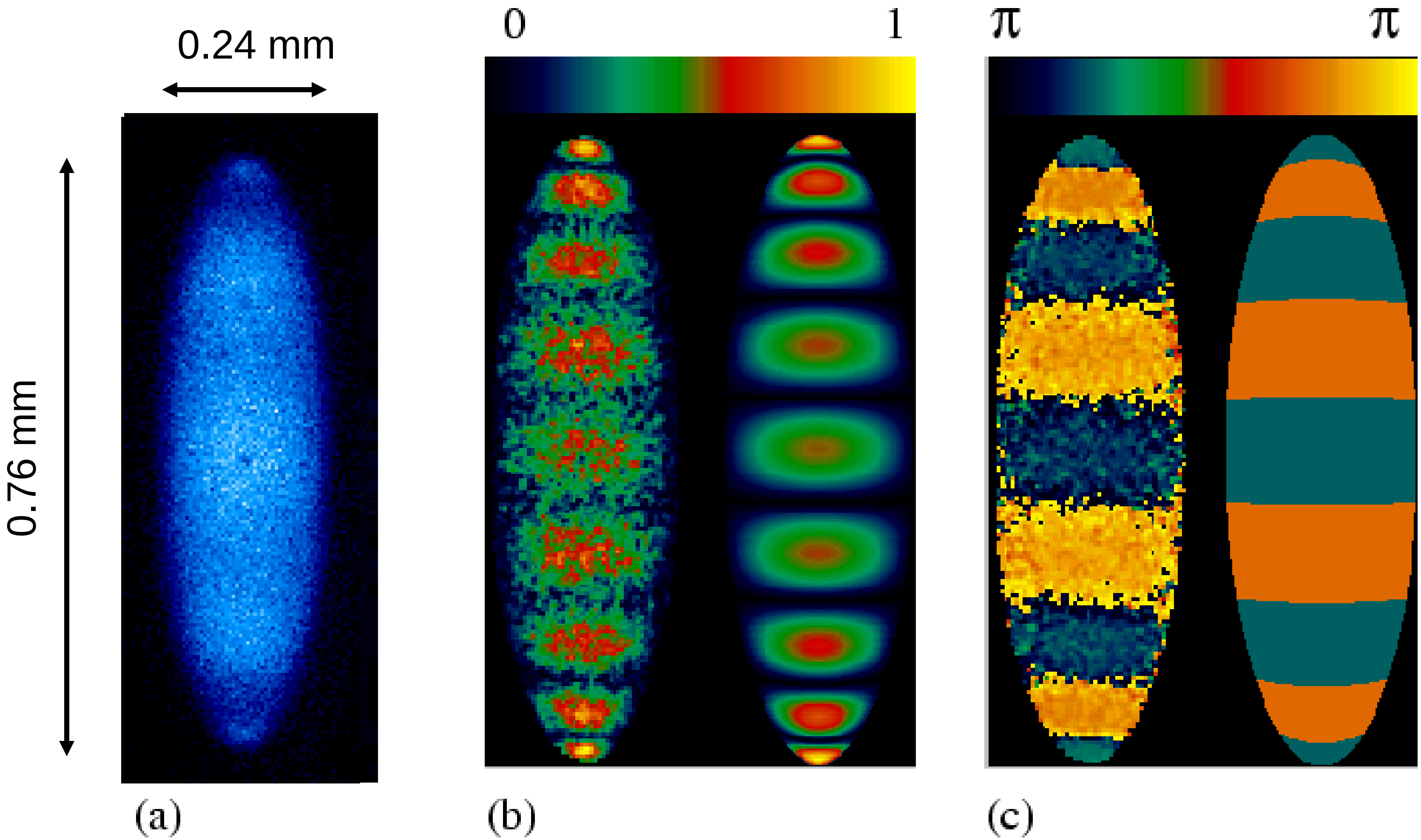

side-view image   mode amplitude   mode phase

Mitchell et al., Optics Express 2, 314 (1998)

l=1 modes excited by static field errors

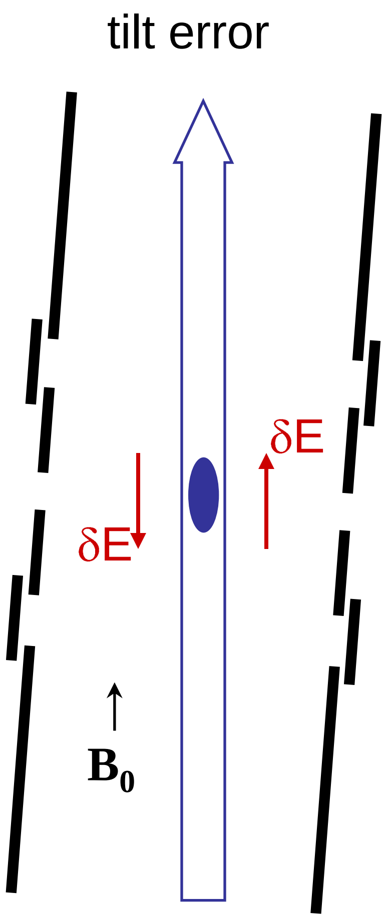

produces a perturbed electric field δE directed down on one side of the trap and up on the other

(4,1)

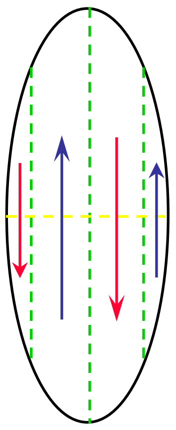

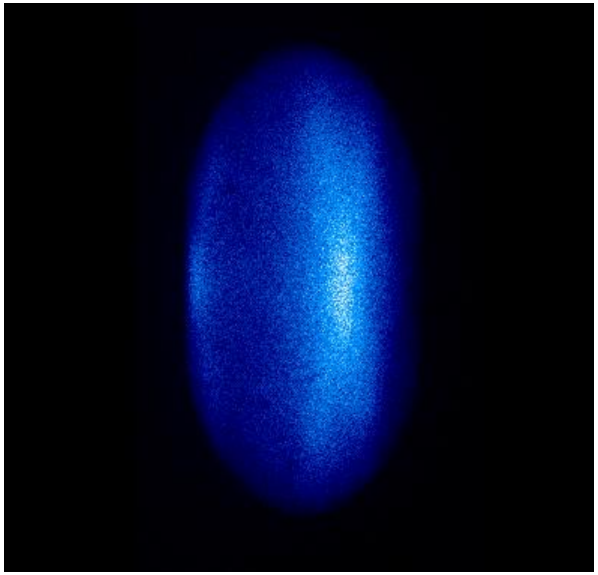

(6,1)

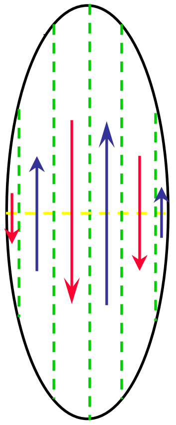

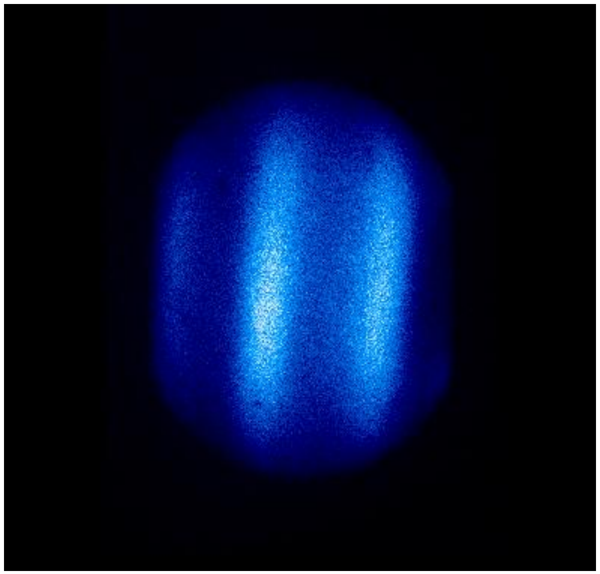

Provides alignment to better than 0.01 degrees !!

Plasma waves excited by laser radiation pressure

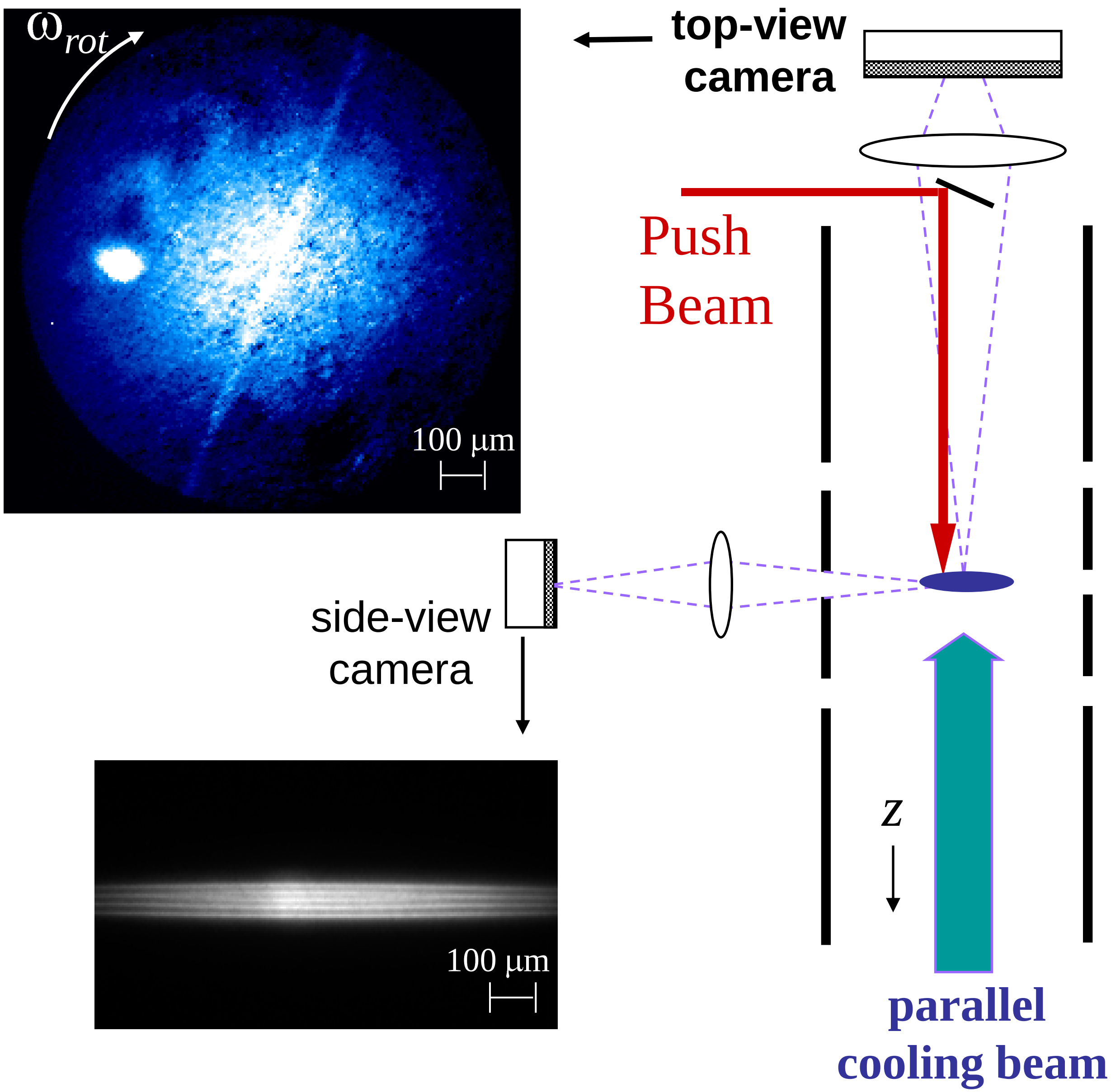

Push on the top of a rotating ion crystal with a laser beam.

The waves which are excited interfere to form a "wake".

Doppler image of wakes

Image w/ push beam

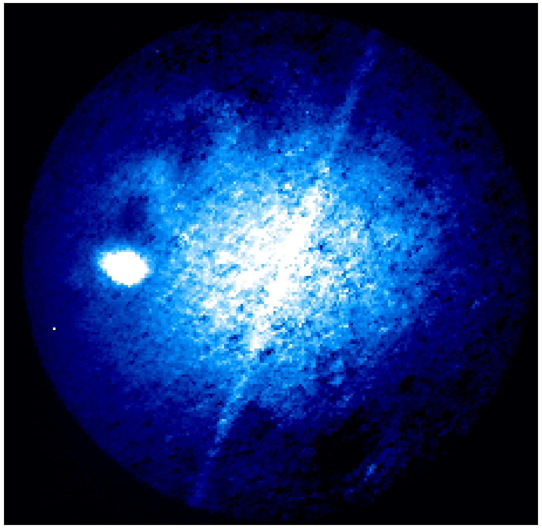

Image w/o push beam

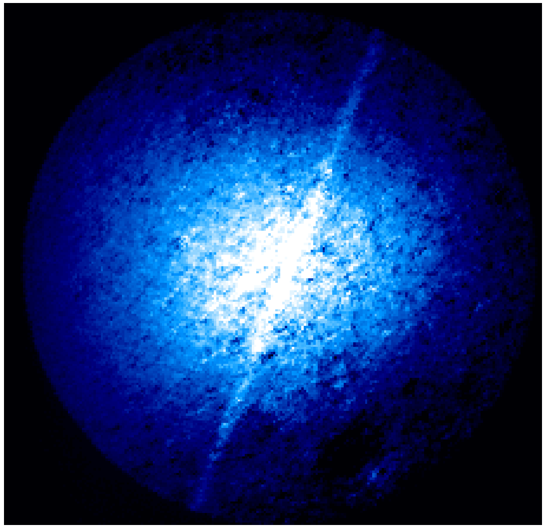

Subtract the two images

Variations in image intensity (shown with a false color scale) correspond to variations in the axial motion of the ions in the crystal.

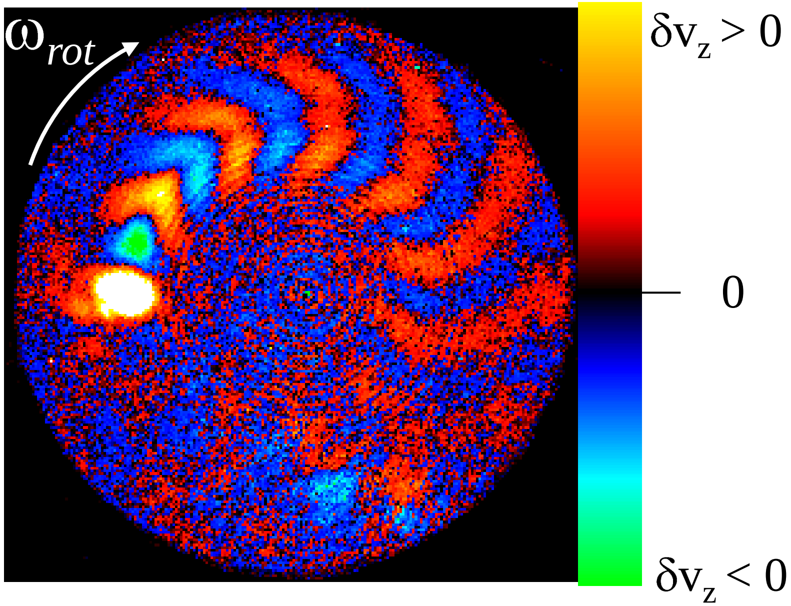

A large spectrum of modes are excited, which interfere to form a wake that is stationary in the source (lab) frame.

Analogous to wakes in water

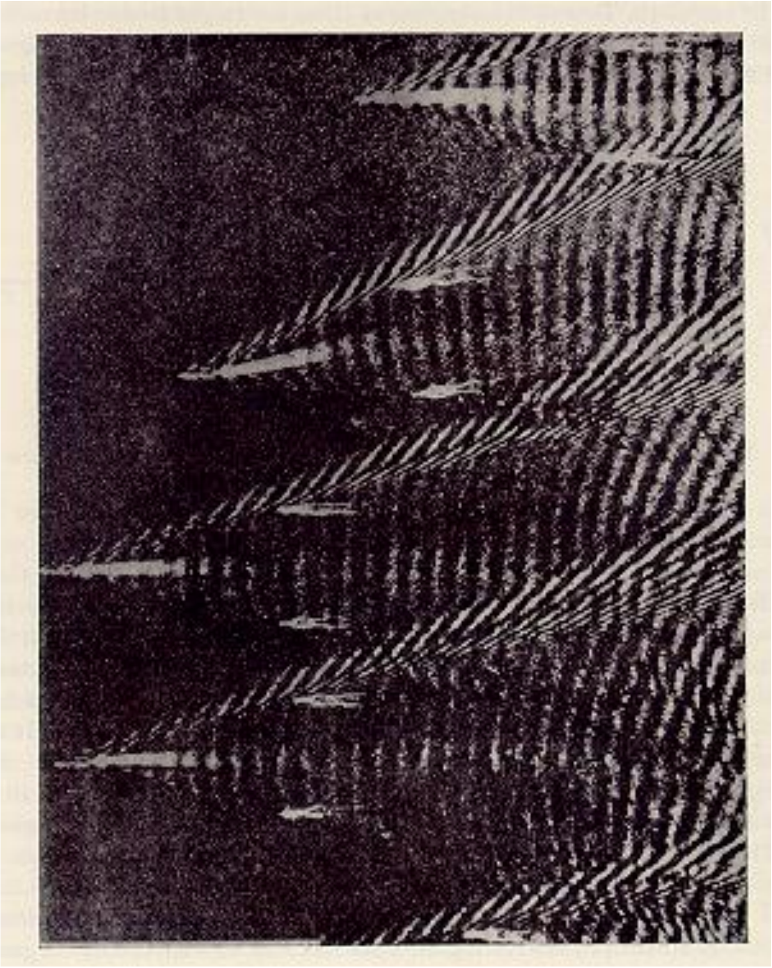

Wakes are Stationary in the frame of the source (ship).

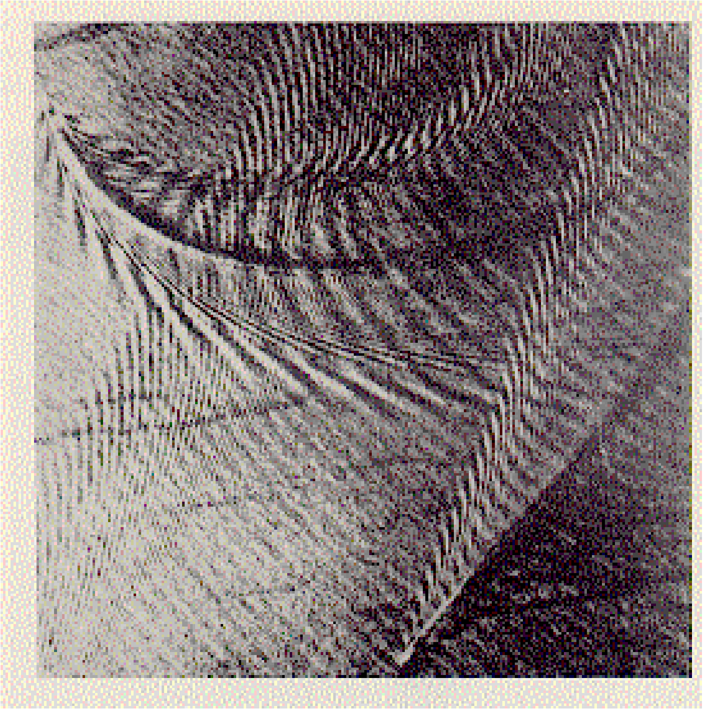

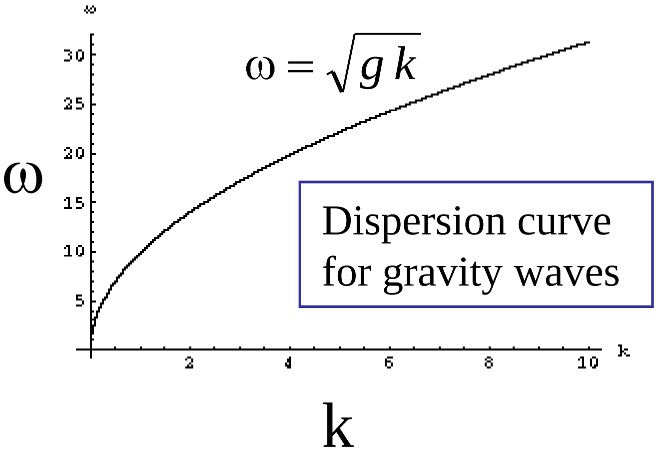

Analyze image to obtain λ and ω

Analyze wake pattern in an annular region that is directly "behind" the push beam.

Fit to damped sinusoid to get λ:

$$y = C_0 + C_1 \,\mathrm{Sin}(C_2 x + C_3)\, e^{-C_4 x}$$

$$C_2 = k = 2\pi/\lambda$$

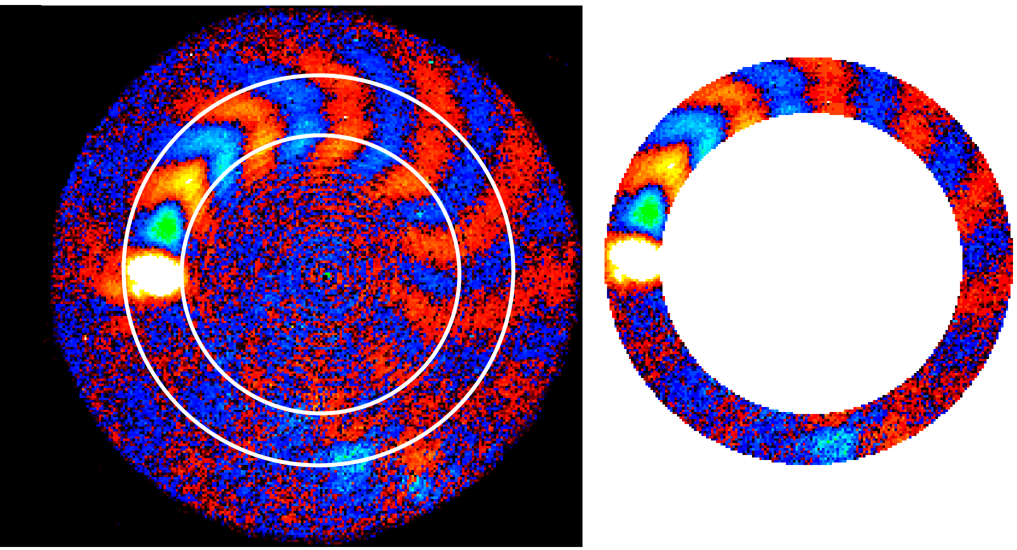

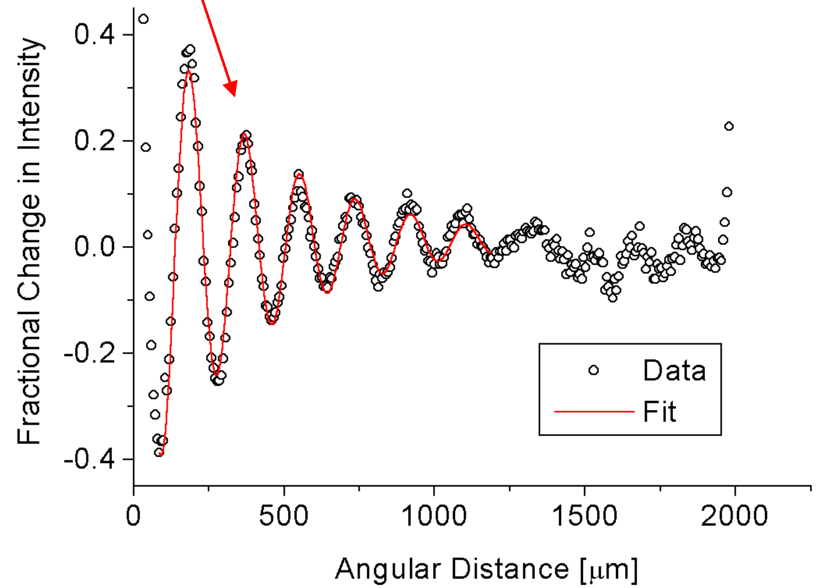

Directly behind the beam, the stationary phase condition gives:

$$v_{source} = \omega_{Rot} r_{source} = \omega/k$$

For this case:

$\lambda = 180\ \mu\text{m}$	$\delta v_z < 1$ m/s
$\omega/2\pi = 500$ kHz	$\delta z < 0.3\ \mu\text{m}$

Dispersion relationship

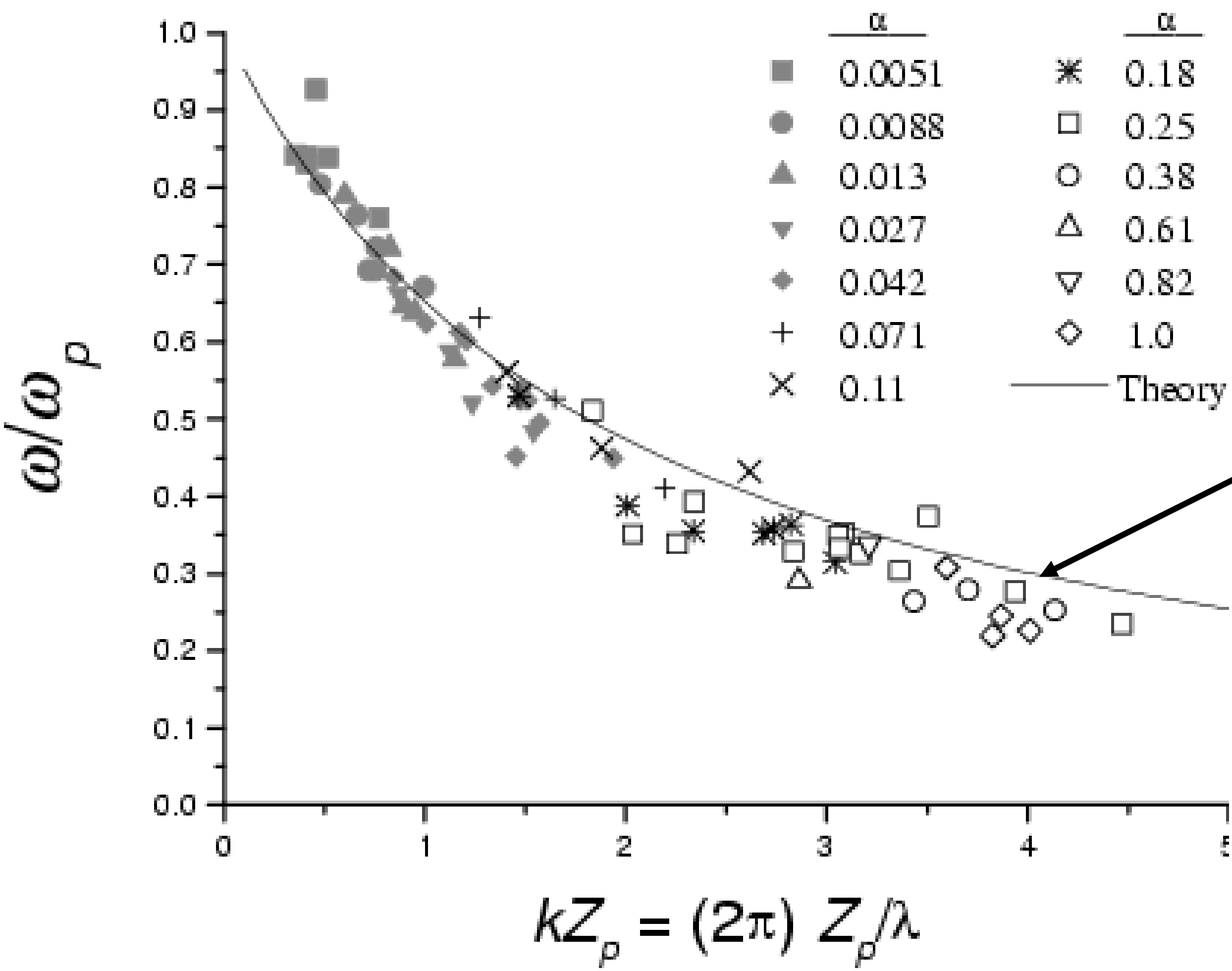

The data agrees with the theoretical dispersion relationship for drumhead waves in a plasma slab of thickness $2Z_p$.

$$\tan\left[\frac{kZ_p}{\sqrt{\omega_p^2/\omega^2-1}}\right]=\sqrt{\omega_p^2/\omega^2-1}$$

Theory replicates experiment

Side View

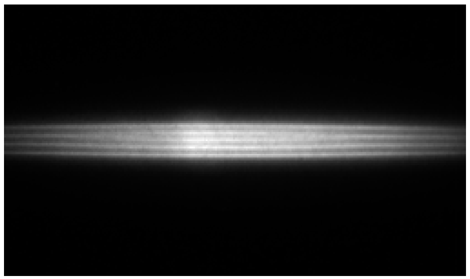

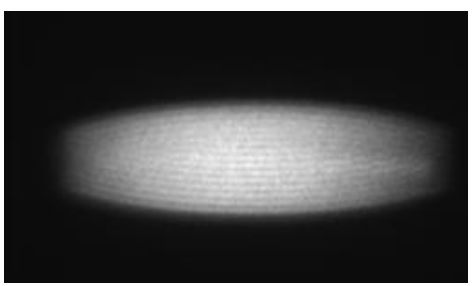

Top View

Experiment

Theory -Dubin

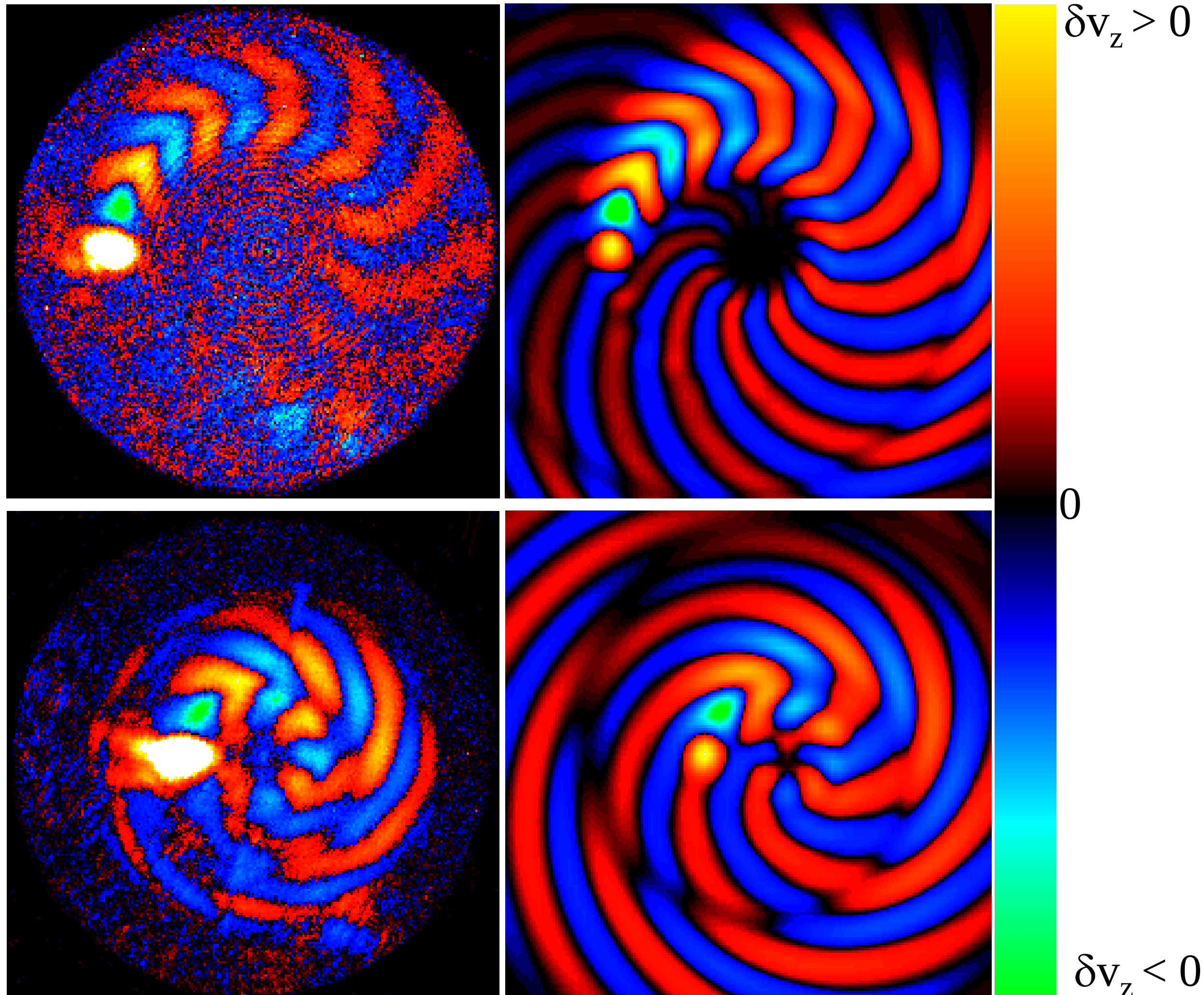

Summary

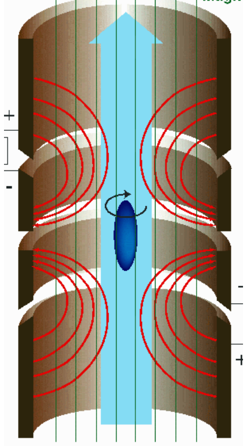

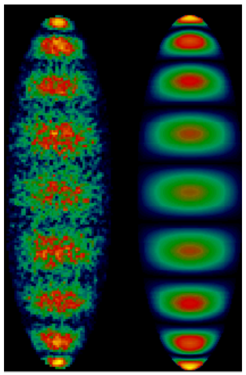

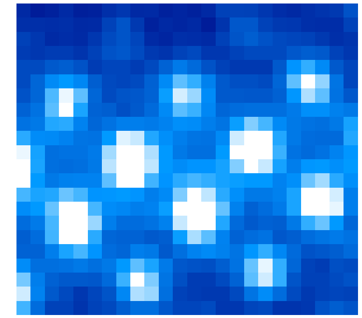

- Penning trap uses static fields for confinement enabling laser cooling of large ion clouds; plasma rotation is required for confinement.

- 2-D and 3-D crystals observed and understood as structures that minimize the Coulomb potential energy

- Long wavelength mode structure can be calculated exactly and precisely understood

Tuesday:

- Quantum information and simulation experiments with 2-D arrays